

NASA TECHNICAL NOTE



NASA TN D-4651

C.1

NASA TN D-4651



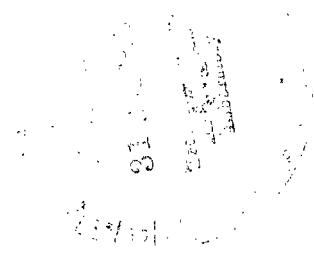
LOAN COPY: RETURN TO
AFWL (WLIL-2)
KIRTLAND AFB, N MEX

DYNAMICS OF A ONE-DIMENSIONAL PLASMA SHEATH

by Frank Hohl and Leo D. Staton

Langley Research Center

Langley Station, Hampton, Va.





0131370

DYNAMICS OF A ONE-DIMENSIONAL PLASMA SHEATH

By Frank Hohl and Leo D. Staton

Langley Research Center
Langley Station, Hampton, Va.

NATIONAL AERONAUTICS AND SPACE ADMINISTRATION

For sale by the Clearinghouse for Federal Scientific and Technical Information
Springfield, Virginia 22151 - CFSTI price \$3.00

DYNAMICS OF A ONE-DIMENSIONAL PLASMA SHEATH*

By Frank Hohl and Leo D. Staton
Langley Research Center

SUMMARY

Analytical and numerical methods are used to investigate a bounded one-dimensional plasma with a fixed neutralizing ion background. A variational method is used to show that a large class of stationary solutions of the nonlinear Vlasov equations represent minimum-energy states. The consequence of the minimum-energy property is that the stationary states, which represent minimum-energy configurations, can never be completely reached. However, numerical experiments which simulate the system reveal the interesting property that the plasma approaches its stationary state closely whenever the initial energy is not too different from the energy of this stationary state.

INTRODUCTION

A one-dimensional model is used to investigate the approach to an equilibrium state (that is, to a state described by a stationary solution of the Vlasov equation) of a bounded plasma with a fixed neutralizing ion background. The stationary states of the system are investigated analytically, and numerical experiments with a charge-sheet model are performed to study the time development of the system. The present problem is different from most previously investigated problems in that the system is strongly inhomogeneous. The fixed neutralizing ion background is constant over a given region and is zero outside this region. The electrons will then form a sheath at each side of the plasma slab.

The usefulness of the one-dimensional sheet model has been well established in plasma physics. Some pioneering work in this field was done by Buneman (refs. 1 and 2). Buneman finds that collective interactions or collisions of charge in bulk can restore a

*The information contained in the text is part of a thesis by Frank Hohl entitled "Collective Effects in Stellar Dynamics and Plasma Physics" offered in partial fulfillment of the requirements for the degree of Doctor of Philosophy in Physics, College of William and Mary, Williamsburg, Virginia, June 1967. The appendix was written by Leo D. Staton.

grossly non-Maxwellian velocity distribution within a few plasma periods to a near-Maxwellian distribution by means of the buildup of electrodynamic instabilities. In similar work, the one-dimensional sheet model has been applied to specific problems by Dunn and Ho (ref. 3), Birdsall and Bridges (refs. 4 and 5), Smith and Dawson (ref. 6), Burger, Dunn, and Halsted (ref. 7), Derfler (ref. 8), and Hasegawa and Birdsall (ref. 9). The same model was used by Burger (refs. 10 and 11) to analyze the stability of direct-current solutions for the plane diode. A discrete one-dimensional computer model for a collisionless plasma in a magnetic field was used by Auer, Hurwitz, and Kilb (refs. 12 and 13) to examine the structure of magnetic compression waves. This work was later extended by Rossow (ref. 14).

Dawson (refs. 15 and 16), and Eldridge and Feix (refs. 17 and 18) initiated a study of the one-dimensional sheet model to check the theoretical predictions of plasma behavior. Dawson (ref. 15) investigated the thermal equilibrium properties of plasmas, such as: the drag on a test particle, Debye shielding, diffusion in velocity space, Landau damping of Fourier modes, and other parameters. In a subsequent paper (ref. 16), Dawson used numerical methods to investigate the thermal relaxation of a one-species one-dimensional plasma and found that there is no relaxation to a Maxwellian to first order (that is, a number of plasma periods equal to the number of particles per Debye length), as was shown analytically by Eldridge and Feix (ref. 19). Eldridge and Feix (refs. 17 and 18) performed numerical experiments to study the properties of the one-dimensional plasma near equilibrium and related some of the one-dimensional plasma properties to the three-dimensional case. The agreement with the theoretical prediction of the results obtained from the numerical experiments gives considerable confidence in the simulation of Vlasov systems by only a few thousand particles.

SYMBOLS

a	acceleration
a_{nm}	matrix elements defined by equation (79)
A	constant, $\frac{N}{4x_0v_0}$
B	constant defined by equation (64)
e	magnitude of electronic charge or charge per unit area
E	electric field

f	electron distribution functions
F	energy distribution function
g	energy density defined by equations (72) and (76)
$g^* = g + 2\lambda B_k V(k)$	
g_T	kinetic-energy density, $\frac{m}{3} B_k V(k)^3$
h	function defined by equation (85)
H	Heaviside unit step function
m	electron mass or mass per unit area
n	density
N	total number of electron charge sheets
P	potential energy
$s = 1 - z$	
t	time
T	kinetic energy
U	total energy of a charge sheet, $\frac{1}{2}mv^2 - e\varphi$
v	velocity
v_T	thermal velocity
V, V_{\pm}	contours defining regions of constant f
w	variable defined by equation (A4b)
W	total system energy, $T + P_e + P_i$

W^*	defined by equation (A5)
x	position coordinate
X, X_1, X_2	positions defined by $V(x) = 0$
z	dimensionless variable, $\frac{Ne^2}{8\epsilon_f\epsilon} x$
α	constant defined by equation (25)
β	constant of integration, $\frac{2A}{n_o} \sqrt{\frac{\pi}{2\kappa m}}$
Γ	defined by equation (A4c)
δ	Dirac delta function or dimensionless energy, $\frac{U}{\epsilon}$
ϵ	maximum energy of an electron defined by equation (38)
ϵ_f	permittivity of free space
ξ	dimensionless position coordinate defined by equations (22) and (49)
η	dummy integration variable
θ	variable defined by equation (70)
κ	thermal energy
λ	Lagrangian multiplier
λ_D	Debye length, $v_T \sqrt{\frac{m\epsilon_f}{n_e e^2}}$
ρ	charge density
σ	charge per unit area
τ	period defined by equation (45)

φ electric potential

Φ dimensionless potential defined by equations (21) and (50)

ω_p plasma frequency, $\frac{n_e e^2}{m \epsilon_f}$

Subscripts:

e electron

eq equilibrium

i ion

j,k,n summation indices

min minimum

o initial

s system boundary

Superscripts:

k summation index defining waterbag contours or ordering index

m,n summation indices

A prime on a symbol indicates partial differentiation with respect to x .

STATIONARY EQUATIONS FOR A BOUNDED PLASMA

The characteristic time for collective effects in a plasma is given by

$$\omega_p^{-1} = \sqrt{\frac{m \epsilon_f}{n_e e^2}} \quad (1a)$$

where e is the charge and m is the mass of an electron. The characteristic length is the Debye length given by

$$\lambda_D = \frac{v_T}{\omega_p} = v_T \sqrt{\frac{m \epsilon_f}{n_e e^2}} \quad (1b)$$

The Vlasov equation for the one-dimensional system with a fixed ion background takes the form

$$\frac{\partial f}{\partial t} + v \frac{\partial f}{\partial x} - \frac{eE}{m} \frac{\partial f}{\partial v} = 0 \quad (2)$$

where $E = -\frac{\partial \varphi}{\partial x}$ and f is the electron distribution function. The electric potential φ is given by the Poisson equation

$$\frac{\partial^2 \varphi}{\partial x^2} = -\frac{e}{\epsilon_f} \left(n_i - \int f \, dv \right) \quad (3)$$

where n_i is the fixed ion density. The integrations are performed over all values of the variables throughout the remainder of the paper, unless otherwise specified. In the steady state, $\frac{\partial f}{\partial t} = 0$ and equation (2) takes the form

$$v \frac{\partial f}{\partial x} - \frac{eE}{m} \frac{\partial f}{\partial v} = v \frac{\partial}{\partial x} + \frac{e}{m} \frac{d\varphi}{dx} \frac{\partial f}{\partial v} = 0 \quad (4)$$

Virial Theorem

In order to obtain a relation between the kinetic and potential energy of the system in equilibrium the identity

$$\frac{m}{2} \frac{D^2}{Dt^2} \int \int x^2 f(x,v) dx \, dv = m \int \int v^2 f(x,v) dx \, dv + m \int \int x a f(x,v) dx \, dv \quad (5)$$

is investigated where

$$\frac{D}{Dt} = \frac{\partial}{\partial t} + v \frac{\partial}{\partial x} + a \frac{\partial}{\partial v} \quad (6)$$

and $\frac{Df}{Dt} = 0$ according to equation (2). Because the system is in equilibrium, the left-hand side of equation (5) is zero. The first term on the right-hand side of equation (5) is $2T$ where T is the expectation value of the kinetic energy of the electron system. The last term of equation (5) is now investigated. By using Newton's law, a can be replaced by $\frac{e}{m} \frac{d\varphi}{dx}$. Also, the electron density is given by

$$n_e = \int f \, dv \quad (7)$$

By using the Poisson equation

$$\frac{d^2\varphi}{dx^2} = -\frac{e}{\epsilon_f}(n_i - n_e) \quad (8)$$

the electron density can be written as

$$n_e = \frac{\epsilon_f}{e} \frac{d^2\varphi}{dx^2} + n_i \quad (9)$$

The last integral of equation (5) can then be written in the form

$$\begin{aligned} m \int \int x f \frac{d^2x}{dt^2} dx dv &= \epsilon_f \int x \frac{d\varphi}{dx} \left(\frac{d^2\varphi}{dx^2} + \frac{e}{\epsilon_f} n_i \right) dx \\ &= \epsilon_f \int x \frac{d\varphi}{dx} \frac{d^2\varphi}{dx^2} dx + e \int n_i x \frac{d\varphi}{dx} dx \end{aligned} \quad (10)$$

An integration by parts gives the result

$$\epsilon_f \int x \frac{d\varphi}{dx} \frac{d^2\varphi}{dx^2} dx = \epsilon_f x \left(\frac{d\varphi}{dx} \right)^2 \Big|_{-x_S}^{x_S} - \epsilon_f \int \left(\frac{d\varphi}{dx} \right)^2 dx - \epsilon_f \int x \frac{d\varphi}{dx} \frac{d^2\varphi}{dx^2} dx \quad (11)$$

or

$$\epsilon_f \int x \frac{d\varphi}{dx} \frac{d^2\varphi}{dx^2} dx = \frac{\epsilon_f}{2} \left[x \left(\frac{d\varphi}{dx} \right)^2 \Big|_{-x_S}^{x_S} - \int \left(\frac{d\varphi}{dx} \right)^2 dx \right] = -P_e \quad (12)$$

where P_e is the potential energy of the electron system and the system is assumed to be

symmetric in x . The term $\frac{\epsilon_f x}{2} \left(\frac{d\varphi}{dx} \right)^2 \Big|_{-x_S}^{x_S}$ in the potential-energy definition is required

to normalize the potential energy if the system contains a net charge or if an externally applied field is present. The last integral in equation (10) must now be considered. An integration by parts gives the result

$$\int_{-x_i}^{x_i} n_i x \frac{d\varphi}{dx} dx = n_i x \varphi \Big|_{-x_i}^{x_i} - \int_{-x_i}^{x_i} n_i \varphi dx = -P_i \quad (13)$$

where x_i defines the boundary of the fixed neutralizing ion background; that is,

$n_i = n_0$ for $-x_i < x < x_i$ and $n_i = 0$ otherwise. The energy P_i is related to the

potential energy of the ion background. In general, the potential energy of a one-dimensional system of charges σ_i is given by

$$P = \frac{1}{2} \sum \varphi_i \sigma_i - \frac{1}{2} \int \rho \varphi dx \quad (14)$$

Because $\varphi = 0$ can always be chosen at $x = x_i$, equation (13) can be put in the same form as equation (14). In the remainder of the paper φ is always taken to be zero at $x = 0$. Only systems with zero net charge are treated so that $x \left(\frac{d\varphi}{dx} \right)^2 \Big|_{-x_s}^{x_s} = 0$, and equation (6) takes the form

$$2T = P_e + P_i \quad (15a)$$

In the limit as $x_i \rightarrow 0$, the system consists of two electron sheaths which are held together by a thin but dense positive charge. The ions then simply take the place of a positively charged grid through which the electrons can pass freely and $P_i = 0$. Equation (15a) then takes the usual form

$$2T = P_e \quad (15b)$$

The total energy of the system is always given by $T + P_e$ and is a constant of the motion.

If the ions are not assumed to be fixed and the ion density is given by an equation similar to equation (7), then

$$2(T_e + T_i) - P = 0 \quad (16)$$

where $P = P_e$ as given by equation (12).

Equilibrium Solutions

By using the method of characteristics to solve equation (4), any distribution function F , which is a function only of U , is found to be a solution of equation (4) where

$$U = \frac{1}{2} mv^2 - e\varphi \quad (17)$$

is the energy of a charge sheet. If an equilibrium state can be reached by starting from a given initial distribution f_0 , then

$$f_0(x, v, t \rightarrow \infty) \rightarrow F(U) \quad (18)$$

The form of $F(U)$ depends on the initial distribution and must, in general, be obtained by following the time development of the nonlinear Vlasov equation. However, if an initial distribution which is constant over a certain region of phase space and is zero outside this region is taken, then $F(U)$ can be obtained without following the evolution of the distribution function. This $F(U)$ is unique. The distribution is shown in figure 1. According to the Vlasov equation, f remains constant along the different trajectories so that the region in phase space can only change its shape with time while its area remains constant. For this reason, this distribution function has been called the waterbag model by DePackh (ref. 20). This model is of interest primarily because there corresponds to it only one possible equilibrium state which is easily calculated and can be used for comparison with the numerical results.

For the waterbag model, $F(U) = A = \text{Constant}$ for $0 \leq U \leq \epsilon$, and $F(U) = 0$ for $U > \epsilon$.

The equilibrium solution for the waterbag model is now obtained. The initial shape of the waterbag is taken to be a rectangle defined by the area in phase space between $\pm x_0$ and $\pm v_0$. The function $F(U)$ is used in the Poisson equation (3) and the integration over dv is changed to an integration over dU . Because the density at a given x is of interest, dv is given by

$$\pm dv = \frac{dU}{\sqrt{2m(U + e\phi)}} \quad (19)$$

The Poisson equation can be written as

$$\begin{aligned} \frac{d^2 \phi}{dx^2} &= -\frac{e}{\epsilon_f} \left(n_i - \frac{2A}{\sqrt{2m}} \int_{-e\phi}^{\epsilon} \frac{dU}{\sqrt{U + e\phi}} \right) \\ &= -\frac{e}{\epsilon_f} \left(n_i - \frac{4A}{\sqrt{2m}} \sqrt{\epsilon + e\phi} \right) \end{aligned} \quad (20)$$

where

$$n_i = n_0 \quad (|x| < |x_1|)$$

and

$$n_i = 0 \quad (|x| > |x_1|)$$

If Φ and ζ are introduced such that

$$\Phi = -\frac{e\varphi}{\epsilon} \quad (21)$$

and

$$\zeta^2 = x^2 \left(\frac{n_0 e^2}{\epsilon \epsilon_f} \right) \quad (22)$$

then equation (20) takes the form

$$\frac{d^2 \Phi}{d\zeta^2} - 1 + \alpha \sqrt{1 - \Phi} = 0 \quad (\zeta < \zeta_i) \quad (23)$$

and

$$\frac{d^2 \Phi}{d\zeta^2} + \alpha \sqrt{1 - \Phi} = 0 \quad (\zeta > \zeta_i) \quad (24)$$

where

$$\alpha = \frac{2A}{n_0} \sqrt{\frac{2\epsilon}{m}} \quad (25)$$

A first integration of equations (23) and (24) yields

$$\left(\frac{d\Phi}{d\zeta} \right)^2 - 2 \left\{ \Phi + \frac{2\alpha}{3} \left[(1 - \Phi)^{3/2} - 1 \right] \right\} = 0 \quad (\zeta < \zeta_i) \quad (26)$$

and

$$\left(\frac{d\Phi}{d\zeta} \right)^2 - \frac{4\alpha}{3} (1 - \Phi)^{3/2} = 0 \quad (\zeta > \zeta_i) \quad (27)$$

respectively. The constants of integration in equations (26) and (27) have been evaluated by using the boundary conditions $\frac{d\Phi}{d\zeta} = 0$ and $\Phi = 0$ at $\zeta = 0$, and $\frac{d\Phi}{d\zeta} = 0$ and $\Phi = 1$ at $\zeta = \zeta_s$ where ζ_s defines the boundary of the system. The first two boundary conditions are obtained by applying symmetry in ζ and the last two are obtained by using overall charge neutrality. Because $\frac{d\Phi}{d\zeta}$ and Φ are continuous at the boundary of the neutralizing ion background ζ_i

$$\Phi(\zeta_i) = \Phi_i = \frac{2\alpha}{3} \quad (28)$$

and a second integration gives the final result

$$\pm\zeta = \int_0^{\Phi} \left\{ 2\eta + \frac{4\alpha}{3} \left[(1-\eta)^{3/2} - 1 \right] \right\}^{-1/2} d\eta \quad (\zeta < \zeta_i) \quad (29)$$

$$\pm\zeta = \zeta_i + \sqrt{\frac{12}{\alpha}} \left[\left(1 - \frac{2\alpha}{3} \right)^{1/4} - (1-\Phi)^{1/4} \right] \quad (\zeta > \zeta_i) \quad (30)$$

where ζ_i is given by equation (29) with the upper limit of the integral equal to Φ_i . The numerical solution of equations (29) and (30) is shown in figure 2 which gives Φ as a function of $\ln \zeta$ for several values of α . Equations (21) and (22) can be used to obtain φ as a function of x . The relation

$$n_0 = \frac{N}{2x_i} \quad (31)$$

where N is the total number of electrons or ions in the system and equation (25) is used to eliminate n_0 and ϵ from equation (22). Then

$$x_i = \left[\left(\frac{\alpha \zeta_i}{4Ae} \right)^2 N m \epsilon_f \right]^{1/3} \quad (32)$$

and the numerical values for n_0 and ϵ are easily obtained. The constant of proportionality in equation (22) is found from the ratio

$$\sqrt{\frac{\epsilon \epsilon_f}{n_0 e^2}} = \frac{x_i}{\zeta_i} \quad (33)$$

where equation (32) is used. Figure 3 shows the variation of the electron density for three values of α for a system with $N = 1000$, $A = 0.25$, and $\epsilon_f = m = e = 1$. The variation of the electric field is shown in figure 4 for corresponding values. The equilibrium contour in phase space $V_{\pm}(x)$ of the waterbag is given by the equation

$$V_+(x) = -V_-(x) = \sqrt{(\epsilon + e\varphi) \frac{2}{m}} \quad (34)$$

and figure 5 shows the equilibrium contours for three values of α . The parameters used in the calculation are the same as those used in figure 4. Equations (29) and (30) cannot be used if the positive ion background reduces to a thin but dense charge and $x_i \rightarrow 0$. Such a system corresponds to a positively charged permeable grid through which

the electrons can pass freely; that is, there are two electron sheaths that are held together by a dense, thin positive charge. The Poisson equation (3) can be written as

$$\frac{d^2\varphi}{dx^2} = \frac{4eA}{\epsilon_f\sqrt{2m}}\sqrt{\epsilon + e\varphi} \quad (x \neq 0) \quad (35)$$

A first integration gives the result

$$\frac{d\varphi}{dx} = -\sqrt{\frac{16A}{3\epsilon_f\sqrt{2m}}}(\epsilon + e\varphi)^{3/4} + \text{Constant} \quad (36)$$

The boundary conditions are that $\frac{d\varphi}{dx} = 0$ and $\varphi = -\frac{\epsilon}{e}$ for $x = x_S$ and that

$\lim_{x \rightarrow 0^+} \frac{d\varphi}{dx} = -\frac{Ne}{2\epsilon_f}$ and $\lim_{x \rightarrow 0^+} \varphi = 0$. By using these boundary conditions, the constant of integration is found to be zero and

$$\frac{d\varphi}{dx} = -\frac{Ne}{2\epsilon_f} \left(1 + \frac{e\varphi}{\epsilon}\right)^{3/4} \quad (37)$$

where

$$\epsilon^{3/4} \sqrt{\frac{16A}{3\epsilon_f\sqrt{2m}}} = \frac{Ne}{2\epsilon_f}$$

so that the maximum energy of an electron is

$$\epsilon = \left(\frac{Ne}{8} \sqrt{\frac{3}{\epsilon_f A}} \sqrt{2m}\right)^{4/3} \quad (38)$$

An integration of equation (37) gives the final result

$$\pm x = \frac{8\epsilon_f\epsilon}{Ne^2} \left[1 - \left(1 + \frac{e\varphi}{\epsilon}\right)^{1/4}\right] \quad (39)$$

Figure 6 shows the variation of $E = -\frac{d\varphi}{dx}$ given by equation (37) as a function of x .

The variation of the period of oscillation of a charge sheet as a function of energy seems to give a measure of the effectiveness of phase (or orbit) mixing for the system. For example, in the problem of a self-gravitating system (ref. 21), the variation of the period with particle energy is very small and the oscillations in the kinetic energy of the system persist for a long time. As is shown subsequently, the variation of the electron period with energy is large for the present problem and the oscillations of the kinetic energy with time quickly damp. Only the period for the case where $x_i = 0$ will be

calculated. The equation of motion for a charge sheet is

$$m \frac{d^2 x}{dt^2} = e \frac{d\phi}{dx} = -e \frac{d\Phi}{dx} \quad (40)$$

By using the normalization given by equation (21), equation (39) (for positive x) can be written as

$$\Phi = 1 - (1 - z)^4 \quad (41)$$

where $z = x \left(\frac{Ne^2}{8\epsilon_f \epsilon} \right)$. Therefore,

$$\frac{d\Phi}{dz} = 4(1 - z)^3 \quad (42)$$

and equation (40) takes the form

$$\frac{d^2 z}{dt^2} + \frac{N^2 e^4}{16m\epsilon_f^2 \epsilon} (1 - z)^3 = 0 \quad (43)$$

A first integration of equation (43) gives the result

$$\left(\frac{dz}{dt} \right)^2 = \frac{N^2 e^4}{32m\epsilon_f^2 \epsilon} \left[(1 - z)^4 - (1 - \delta) \right] \quad (44)$$

where $\delta = \frac{U}{\epsilon}$ and U is the total energy of the sheet under consideration. A second integration of equation (43) gives the period of oscillation as

$$\begin{aligned} \tau &= \frac{16\epsilon_f}{Ne^2} \sqrt{2m\epsilon} \int_0^{1-(1-\delta)^{1/4}} \left[(1 - z)^4 - (1 - \delta) \right]^{-1/2} dz \\ &= \frac{16\epsilon_f}{Ne^2} \sqrt{2m\epsilon} \int_{(1-\delta)^{1/4}}^1 \left[s^4 - (1 - \delta) \right]^{-1/2} ds \end{aligned} \quad (45)$$

where $s = 1 - z$ and the limits of integration are found from equation (44) by setting

$\frac{dx}{dt} = 0$. The variation of the electron period as a function of energy is shown in figure 7.

The time τ_0 has been arbitrarily chosen. Because of the strongly nonlinear restoring force $eE(x)$, the variation of the period from zero to infinity is not surprising. For the case where x_i is not zero, the period approaches infinity as U approaches ϵ .

The stationary state for a system which is described by a distribution function

$$F(U) = A \exp(-\kappa U) \quad (46)$$

is easily obtained by the same method as that used for the waterbag model. The solution is given by

$$\zeta = \int_0^\Phi \left\{ 2 \left[\eta + \beta \exp(-\eta) \right] - 2\beta \right\}^{-1/2} d\eta \quad (\zeta < \zeta_i) \quad (47)$$

and

$$\zeta = \sqrt{\frac{2}{\beta}} \left[\exp\left(\frac{\Phi}{2}\right) - \exp\left(\frac{\beta}{2}\right) \right] + \zeta_i \quad (\zeta > \zeta_i) \quad (48)$$

where $\beta = \frac{2A}{n_0} \sqrt{\frac{\pi}{2\kappa m}}$. Also,

$$\zeta^2 = \frac{e^2 n_0 \kappa}{\epsilon_f} \quad (49)$$

and

$$\Phi = -e\varphi\kappa \quad (50)$$

were used. All but one of the constants of integration can be directly evaluated by using the boundary conditions $\frac{d\Phi}{d\zeta} = 0$ and $\Phi = 0$ at $\zeta = 0$, $\lim_{\zeta \rightarrow \infty} \frac{d\Phi}{d\zeta} = 0$, and continuity of $\frac{d\Phi}{d\zeta}$ at $\zeta = \zeta_i$. The equation for $\zeta > \zeta_i$ is then integrated by assuming that the constant is nonzero. In order to satisfy $\lim_{\zeta \rightarrow \infty} \frac{d\Phi}{d\zeta} = 0$, the integration constant must be zero, and equation (48) is obtained. For the case $x_i = 0$, the solution is

$$x = \frac{4\epsilon_f}{N\kappa e^2} \left[\exp\left(\frac{\Phi}{2}\right) - 1 \right] \quad (51)$$

or

$$\Phi = 2 \ln \left(1 + \frac{N\kappa e^2}{4\epsilon_f} x \right) \quad (52)$$

The constants of integration have been evaluated by using the boundary condition

$\lim_{x \rightarrow \infty} \frac{d\Phi}{dx} = 0$, $\lim_{x \rightarrow 0} \frac{d\Phi}{dx} = \frac{Ne^2\kappa}{2\epsilon_f}$, and $\Phi = 0$ at $x = 0$. The condition $\lim_{x \rightarrow 0} \frac{d\Phi}{dx} = \frac{Ne^2\kappa}{2\epsilon_f}$ is

obtained by applying Gauss' theorem to the positive charge sheets at the origin. The electron density corresponding to equation (51) is

$$n_e(x) = \frac{N^2 e^2 \kappa}{8 \epsilon_f} \left(1 + \frac{N e^2 \kappa}{4 \epsilon_f} x \right)^{-2} \quad (53)$$

Figure 8 shows $\Phi(x)$ and $E(x)$ for the case where $x_1 = 0$, $\epsilon_f = 1$, $\kappa = 1$, $e = 1$, and $N = 4$. The electric field is very similar to that for the waterbag case. Thus, irrespective of the exact form of the distribution function, similar evolution of the system might be expected.

MINIMUM-ENERGY PRINCIPLE

The stationary solution for the initial waterbag distribution was obtained by conserving only area in phase space. The stationary (or equilibrium) state is described by a function which depends only on the energy U . For the waterbag model, a unique $F(U)$ corresponding to a given initial energy and particle number can be obtained. Before such an $F(U)$ can be reached, energy considerations must allow the relaxation from a function $f(x, v, t = 0)$ of two independent variables to a function $F(U)$ of the energy only. If an equilibrium state is to be reached, the initial and final energy of the system must be equal. For the initial rectangular waterbag, the kinetic energy T is given by

$$\begin{aligned} T(t = 0) &= \int \int \frac{1}{2} m v^2 f(x, v, t = 0) dx dv \\ &= \frac{Nm}{8x_0 v_0} \int_{-x_0}^{x_0} \int_{-v_0}^{v_0} v^2 dv dx \\ &= \frac{Nm}{6} v_0^2 \end{aligned} \quad (54)$$

As previously stated, $\pm v_0$ and $\pm x_0$ define the rectangular area of the initial distribution. For positive x , the electric field is given by

$$E(x) = \frac{Ne}{2\epsilon_f} \left(\frac{1}{x_1} - \frac{1}{x_0} \right) x \quad (x < x_1) \quad (55)$$

and

$$E(x) = \frac{Ne}{2\epsilon_f} \left(1 - \frac{x}{x_0} \right) \quad (x_1 < x < x_0) \quad (56)$$

and, therefore, the initial potential energy is

$$\begin{aligned} P_e(t = 0) &= \epsilon_f \int_0^{x_0} E^2(x) dx \\ &= \frac{e^2 N^2}{12 \epsilon_f x_0} (x_0 - x_i)^2 \end{aligned} \quad (57)$$

Again, $\pm x_0$ and $\pm v_0$ define the rectangular area of the initial distribution. The total energy of the initial distribution is given by

$$\begin{aligned} W(t = 0) &= T(t = 0) + P_e(t = 0) \\ &= \frac{N}{6} \left[m v_0^2 + \frac{N e^2}{2 x_0 \epsilon_f} (x_0 - x_i)^2 \right] \end{aligned} \quad (58)$$

The minimum value that equation (58) can attain for a given value of $A = \frac{N}{4 x_0 v_0}$ is given by

$$W_{\min}(t = 0) = \frac{N m}{2} \left(\frac{N^2 e^2}{16 A \epsilon_f m} \right)^{2/3} \quad (59)$$

where $x_i = 0$.

By using equations (37) and (38), the potential energy of the equilibrium state for $x_i = 0$ is given by

$$\begin{aligned} P_{eq} &= \frac{\epsilon_f}{2} \int \left(\frac{d\varphi}{dx} \right)^2 dx \\ &= \frac{16 \epsilon_f^2}{7 e} \sqrt{\frac{A \epsilon_f}{3 \sqrt{2 m \epsilon}}} \end{aligned} \quad (60)$$

The kinetic energy is given by

$$\begin{aligned} T_{eq} &= 4 \int_0^{x_s} \int_0^{V_+(x)} \frac{1}{2} m v^2 A dv dx \\ &= \frac{8 \epsilon_f^2}{7 e} \sqrt{\frac{A \epsilon_f}{3 \sqrt{2 m \epsilon}}} \end{aligned} \quad (61)$$

where $V_+(x)$ is given by equation (34). After using equation (38) and $A = \frac{N}{4x_0 v_0}$ to eliminate ϵ and A from equations (60) and (61), the expression for the total energy of the equilibrium state becomes

$$W_{eq} = T_{eq} + P_{eq}$$

$$= \frac{3(9^{1/3})}{7} \left[\frac{Nm}{2} \left(\frac{N^2 e^2}{16 \epsilon_f m} \right)^{2/3} \right] \quad (62)$$

The ratio of equation (59) to the total equilibrium is

$$\frac{W_{min}(t=0)}{W_{eq}} = 1.16 \quad (63)$$

and the initial rectangular distribution with the smallest possible energy has still more energy than the equilibrium distribution. The equilibrium waterbag distribution for a plasma sheath may have, therefore, a minimum-energy property.

The minimum-energy property for the stationary solutions of a plasma sheath represented by a single waterbag is given in the appendix. This property can be shown to hold for a large class of distribution functions that can be described by multiple-contour waterbag distributions. The waterbag model illustrated in figure 9 is used in the analysis. The contours $V_+^{(k)}(x,t)$ and $V_-^{(k)}(x,t)$ describe surfaces of constant $f = f_k$. According to the Vlasov equation, f behaves like an incompressible phase fluid; therefore, the area bounded by any pair of contours is constant. With a large number of contours, the waterbag model can be used to approximate arbitrary distribution functions.

The function

$$f = \sum_k B_k \left\{ H[v - V_-^{(k)}] - H[v - V_+^{(k)}] \right\} \quad (64)$$

describes the waterbag distribution where the summation is over all contours and $H(z)$ is the Heaviside unit step function. The distribution function f , as given by equation (64), satisfies the Vlasov equation

$$\frac{\partial f}{\partial t} + v \frac{\partial f}{\partial x} - \frac{eE}{m} \frac{\partial f}{\partial v} = \sum_k B_k \left\{ \delta[v - V_+^{(k)}] \left[\frac{\partial V_+^{(k)}}{\partial t} + v \frac{\partial V_+^{(k)}}{\partial x} + \frac{eE}{m} \right] \right.$$

$$\left. - \delta[v - V_-^{(k)}] \left[\frac{\partial V_-^{(k)}}{\partial t} + v \frac{\partial V_-^{(k)}}{\partial x} + \frac{eE}{m} \right] \right\} = 0 \quad (65)$$

where $\delta(z)$ is the Dirac delta function. The electric field E is obtained from the equation

$$\frac{dE}{dx} = \frac{e}{\epsilon_f} \left(n_i - \int f dv \right) = \frac{e}{\epsilon_f} \left\{ n_i - \sum_k B_k \left[V_+^{(k)} - V_-^{(k)} \right] \right\} \quad (66)$$

where there is assumed to be a total of N electrons each of charge e in the system. If equation (65) is integrated separately over positive and negative velocity

$$\sum_k B_k \left[\frac{\partial V_+^{(k)}}{\partial t} + V_+^{(k)} \frac{\partial V_+^{(k)}}{\partial x} + \frac{eE}{m} \right] = 0 \quad (67a)$$

and

$$\sum_k B_k \left[\frac{\partial V_-^{(k)}}{\partial t} + V_-^{(k)} \frac{\partial V_-^{(k)}}{\partial x} + \frac{eE}{m} \right] = 0 \quad (67b)$$

The stationary contours are described by

$$\sum_k B_k \left[V_{\pm}^{(k)} \frac{\partial V_{\pm}^{(k)}}{\partial x} + \frac{eE}{m} \right] = 0 \quad (68)$$

which must hold term-by-term. In order to simplify the equations, symmetric contours $V_+^{(k)} = -V_-^{(k)} = V^{(k)}$ are assumed in the remainder of the analysis. The results obtained are not affected by such an assumption. Equation (68) can then be simplified as

$$V^{(k)} \frac{dV^{(k)}}{dx} + \frac{eE}{m} = 0 \quad (69)$$

A new variable is now defined as

$$\left. \begin{aligned} \theta^{(k)}(x) &= 0 & \left(x < x_S^{(k)} \right) \\ \theta^{(k)}(x) &= \int_{-x_S^{(k)}}^x V^{(k)}(\xi) d\xi & \left(-x_S^{(k)} \leq x \leq x_S^{(k)} \right) \\ \theta^{(k)}(x) &= \theta^{(k)}[x_S^{(k)}] & \left(x > x_S^{(k)} \right) \end{aligned} \right\} \quad (70)$$

where $\pm x_s^{(k)}$ are the end points of the k th contour. In terms of $\theta^{(k)}$ the electric field is given by the equation

$$E(x) = \frac{en_0}{\epsilon_f} \left\{ x \left[H(x + x_i) - H(x - x_i) \right] + x_i \left[H(x + x_i) - H(x - x_i) \right] \right\} - \frac{2e}{\epsilon_f} \sum_k B_k \theta^{(k)} \quad (71)$$

The energy density of the system can be represented by a function $g[x, \theta^{(k)}, V^{(k)}]$. The total energy of the system is then given by

$$W = \sum_k \int_{-x_s^{(k)}}^{x_s^{(k)}} g[x, \theta^{(k)}, V^{(k)}] dx \quad (72)$$

For the integral for W to be an extremum subject to the condition that

$$N = \sum_k 2B_k \theta^{(k)} [x_s^{(k)}] \quad (73)$$

is a constant requires that the contours $V^{(k)}$ satisfy the Euler-Lagrange equation

$$\frac{\partial g^*}{\partial \theta^{(k)}} - \frac{d}{dx} \frac{\partial g^*}{\partial V^{(k)}} = 0 \quad (74)$$

where $g^* = g + \lambda 2B_k V^{(k)}$ and λ is an undetermined Lagrangian multiplier. Because the end points $\pm x_s^{(k)}$ are fixed, the constraint on the number of particles is redundant and $\lambda \approx 0$. If the end points $\pm x_s^{(k)}$ are not held fixed in the variational process, additional equations which occur do not change the main results.

For a multiple waterbag, the kinetic energy per unit length is given by

$$\sum_k g_T [V^{(k)}] = \sum_k \frac{m}{3} B_k V^{(k)3} \quad (75)$$

The expression for g then takes the form

$$\begin{aligned}
\sum_{\mathbf{k}} g \left[\mathbf{x}, V^{(\mathbf{k})}, \theta^{(\mathbf{k})} \right] &= \sum_{\mathbf{k}} \frac{B_{\mathbf{k}}^m}{3} V^{(\mathbf{k})^3} + \frac{\epsilon_f}{2} \left(\frac{en_0}{\epsilon_f} \left\{ \mathbf{x} \left[\bar{H}(\mathbf{x} + \mathbf{x}_i) - H(\mathbf{x} - \mathbf{x}_i) \right] \right. \right. \\
&\quad \left. \left. + \mathbf{x}_i \left[\bar{H}(\mathbf{x} + \mathbf{x}_i) - H(\mathbf{x} - \mathbf{x}_i) \right] \right\} - \frac{2e}{\epsilon_f} \sum_{\mathbf{k}} B_{\mathbf{k}} \theta^{(\mathbf{k})} \right)^2 \\
&= \sum_{\mathbf{k}} \frac{B_{\mathbf{k}}^m}{3} V^{(\mathbf{k})^3} - 2e \sum_{\mathbf{k}} B_{\mathbf{k}} \theta^{(\mathbf{k})} \left(\frac{en_0}{\epsilon_f} \left\{ \mathbf{x} \left[\bar{H}(\mathbf{x} + \mathbf{x}_i) - H(\mathbf{x} - \mathbf{x}_i) \right] \right. \right. \\
&\quad \left. \left. + \mathbf{x}_i \left[\bar{H}(\mathbf{x} + \mathbf{x}_i) - H(\mathbf{x} - \mathbf{x}_i) \right] \right\} - \frac{e}{\epsilon_f} \sum_{\mathbf{k}} B_{\mathbf{k}} \theta^{(\mathbf{k})} \right) \\
&\quad + \frac{\epsilon_f}{2} \left(\frac{en_0}{\epsilon_f} \right)^2 \left\{ \mathbf{x} \left[\bar{H}(\mathbf{x} + \mathbf{x}_i) - H(\mathbf{x} - \mathbf{x}_i) \right] \right. \\
&\quad \left. \left. + \mathbf{x}_i \left[\bar{H}(\mathbf{x} + \mathbf{x}_i) - H(\mathbf{x} - \mathbf{x}_i) \right] \right\}^2
\end{aligned} \tag{76a}$$

Because the last term in equation (76a) does not depend on the function $V^{(\mathbf{k})}$ or $\theta^{(\mathbf{k})}$, it can be omitted and g is thus given by

$$\begin{aligned}
\sum_{\mathbf{k}} g \left[\mathbf{x}, V^{(\mathbf{k})}, \theta^{(\mathbf{k})} \right] &= \sum_{\mathbf{k}} \frac{B_{\mathbf{k}}^m}{3} V^{(\mathbf{k})^3} - 2e \sum_{\mathbf{k}} B_{\mathbf{k}} \theta^{(\mathbf{k})} \left(\frac{en_0}{\epsilon_f} \left\{ \mathbf{x} \left[\bar{H}(\mathbf{x} + \mathbf{x}_i) - H(\mathbf{x} - \mathbf{x}_i) \right] \right. \right. \\
&\quad \left. \left. + \mathbf{x}_i \left[\bar{H}(\mathbf{x} + \mathbf{x}_i) - H(\mathbf{x} - \mathbf{x}_i) \right] \right\} - \frac{e}{\epsilon_f} \sum_{\mathbf{k}} B_{\mathbf{k}} \theta^{(\mathbf{k})} \right)
\end{aligned} \tag{76b}$$

The Euler-Lagrange equations then become

$$2B_{\mathbf{k}} \left[m V^{(\mathbf{k})} \frac{dV^{(\mathbf{k})}}{dx} + eE \right] = 0 \tag{77}$$

or

$$V^{(\mathbf{k})} \frac{dV^{(\mathbf{k})}}{dx} + \frac{eE}{m} = 0 \tag{78}$$

which is the equation for the equilibrium contours.

If equation (78) is to represent a minimum-energy configuration, then Legendre's criterion of the second variation of g must be satisfied. The Legendre condition (ref. 22) for the case of several unknown functions $\theta^{(k)}$ is that the quadratic form the coefficient matrix of which has the elements

$$a_{nm} = \frac{\partial^2 g}{\partial V^{(n)} \partial V^{(m)}} \quad (79)$$

must not be negative. For the present problem, only the diagonal elements of equation (79) are nonzero and are given by

$$a_{kk} = 2mB_k V^{(k)} \quad (80)$$

Because $2mV^{(k)}$ is never negative, the Legendre condition requires that

$$B_k > 0 \quad (81)$$

The form of f given by equation (64) shows that the condition $B_k > 0$ is equivalent to stating that the distribution function must decrease monotonically in going outward from the center of the system where $f = f_k = f_1$ must be the largest. If equation (81) is satisfied, the system is not a maximum-energy configuration but is a minimum-energy configuration which is therefore stable. However, if $B_k > 0$ is not satisfied for all k , the system is not a minimum-energy configuration and nothing can be said about its stability.

If the distribution of ions is not fixed but is given by an f similar to equation (64), the system is found to be a minimum-energy configuration when both the electron and ion distribution functions are monotonically decreasing in going outward from the center of the system.

For the case of a single-contour waterbag, the Legendre criterion is always satisfied and the stationary solution represents a minimum-energy configuration which is inaccessible for arbitrary initial distribution. However, the results of numerical experiments show that the system approaches the equilibrium state closely whenever the initial energy is not too far from the energy of the corresponding stationary state. The single-contour waterbag is treated in detail in the appendix.

THE ONE-DIMENSIONAL PLASMA MODEL

The plasma model consists of a system of N ions and N electrons that are represented by $2N$ charge sheets. The charge sheets move only in the x -direction and

are of infinite extent in two transverse directions. When two sheets meet, they are allowed to pass freely through each other. The equations of motion of all the $2N$ sheets are solved simultaneously by computing the position of each sheet and by integrating the equations of motion of each sheet over a small time interval Δt . The equation of motion of a sheet with charge σ_j and mass m_j per unit area is given by

$$\frac{d^2 x_j(t)}{dt^2} = \frac{\sigma_j}{m_j} E_j \quad (82)$$

where x_j is the position of the sheet. The electric field is given by

$$\begin{aligned} \frac{\partial E(x,t)}{\partial x} &= \frac{1}{\epsilon_f} \rho(x,t) \\ &= \sum_{i=1}^{2N} \frac{\sigma_i}{\epsilon_f} \delta[x - x_i(t)] \end{aligned} \quad (83)$$

The magnetic field induced by the charge sheets is neglected. The electric field is then given by

$$E(x,t) = \frac{1}{2\epsilon_f} \sum \sigma_i h[x - x_i(t)] \quad (84)$$

where

$$\left. \begin{aligned} h(z) &= 1 & (z > 0) \\ h(z) &= 0 & (z = 0) \\ h(z) &= -1 & (z < 0) \end{aligned} \right\} \quad (85)$$

In obtaining equation (84), the electric field is assumed to be zero outside the system. For the numerical calculations, the electric field acting on a particular sheet is obtained by the net charge to the left of the sheet x_j ; thus

$$E_j = \frac{1}{\epsilon_f} \left[\sum_{k=1}^{j-1} \sigma^{(k)} - \frac{1}{2} \sigma_j \right] \quad (86)$$

where the superscript k gives the order of the charge sheet $x_j^{(k)}$ such that

$$x^{(k)} \leq x^{(k+1)} \quad (87)$$

The IBM 7094 electronic data processing system was used to calculate the self-consistent motion of systems containing several thousand charge sheets. The position and velocity of each sheet are computed at successive times $t_1, t_2, t_3, \dots, t_m$. For each time step $\Delta t = t_{n+1} - t_n$, the new positions and velocities of the sheets are computed from the equations

$$x_i(t_{n+1}) = x_i(t_n) + \frac{dx_i(t_n)}{dt} \Delta t + \frac{1}{2} \frac{d^2 x_i(t_n)}{dt^2} (\Delta t)^2 \quad (88)$$

and

$$\frac{dx_i(t_{n+1})}{dt} = \frac{dx_i(t_n)}{dt} + \frac{d^2 x_i(t_n)}{dt^2} \Delta t + \frac{1}{2} \frac{d^3 x_i(t_n)}{dt^3} (\Delta t)^2 \quad (89)$$

where

$$\frac{d^2 x_i(t_n)}{dt^2} = \frac{\sigma_i}{\epsilon_f m_i} \left[\sum_{k=1}^{j-1} \sigma^{(k)} - \frac{1}{2} \sigma_j \right] \quad (90)$$

and

$$\frac{d^3 x_i(t_n)}{dt^3} = \frac{1}{\Delta t} \left[\frac{d^2 x_i(t_n)}{dt^2} - \frac{d^2 x_i(t_{n-1})}{dt^2} \right] \quad (91)$$

The kinetic energy of the system is given by

$$T = \sum_{j=1}^{2N} \frac{m_j}{2} \left(\frac{dx_j}{dt} \right)^2 \quad (92)$$

and the potential energy is

$$P = \frac{\epsilon_f}{2} \sum_{j=1}^{2N-1} (x_{j+1} - x_j) E_j^2 \quad (93)$$

NUMERICAL RESULTS

All numerical computations for the sharply bounded plasma were performed for the case where the ratio of the ion mass to electron mass is so large that the ions can be assumed fixed and only the motion of the electrons needs to be calculated. The problem is that of determining the evolution of the electron distribution function for a fixed ion background between $-x_i$ and x_i . The case where x_i is near zero is investigated first. The case corresponds to that of a permeable grid which is positively charged and through which the electrons can pass freely; that is, there are two electron sheaths held together by a thin but dense positive charge. For all calculations, $e = \epsilon_f = m = 1$ is chosen. Figure 10 shows the variation of kinetic energy for a 1000-electron system. The ratio of the initial energy to the equilibrium energy, as given by equation (71), is 1.3. The dashed line shown in figure 10 corresponds to one-third of the total energy of the system and is the kinetic energy given by the virial theorem. The kinetic energy quickly approaches this value. The plasma frequency ω_{po} corresponds to the initial electron density. One important indicator of the approach to an equilibrium state is the time development of the energy distribution function. Figure 11 shows that, after about six plasma periods ($2\pi\omega_{po}^{-1}$), the energy distribution function has approached the equilibrium distribution indicated by the dashed line. After six plasma periods, the system changes very little as its evolution is followed for a longer time. The high-energy tail of the distribution does not disappear and is required to conserve the energy of the system. The corresponding time development of the density is shown in figure 12. The time development of the density indicates that the density of the system quickly tends to approach its equilibrium value as indicated by the continuous curve. The dimension of the sheath at each side of the system is of the order of a Debye length so that the number of particles per Debye length is of the order of the number of particles in the system. Dawson (ref. 16) has shown that thermalization in a uniform one-dimensional plasma occurs only on a time scale $(n\lambda_D)^2\omega_p^{-1}$. Graininess effects in the present system can be expected to become important only after 10^6 plasma periods. The results shown in figure 12 are for times much less than $(n\lambda_D)^2\omega_p$ and are therefore not affected by graininess. The electric field at $t = 30\omega_{po}^{-1}$ is compared with the equilibrium field in figure 13. Because of the high-energy electrons, the electric field of the system does not go to zero as quickly as the equilibrium value. The time development of the system in phase space is shown in figure 14. The system quickly develops arms which wind around the main body of the system as it rotates in phase space. Because of the very long period of rotation for particles at the outer boundary of the system, the arms stretch rather quickly. The calculations in figure 14 are repeated for a 2000-electron system. The results are almost identical and only the initial time development of the system in phase space is shown in figure 15.

Calculation for values of $x_i \neq 0$ are also performed. The dimensions of the sheaths which form at each side of the positive ion background are of the order of a Debye length. For appreciable values of x_i , most of the electrons are in the main body of the plasma, and the number of electrons in the sheath or per Debye length becomes quite small. For moderate values of x_i , graininess effects become very important and the system approaches a Maxwellian distribution. Figure 16 shows the variation of the kinetic energy for a 1000-electron system with $x_i = 477$. Figure 17 shows the time development of the energy distribution function for a collision-dominated system and shows that the system quickly approaches the Maxwellian distribution as indicated by the dashed-line curve. The corresponding results for the time development of the system in phase space are shown in figure 18. Figure 18 indicates that at $t = 45.00\omega_{po}^{-1}$ the Vlasov character of the system has been lost and the system cannot be considered collisionless; therefore, the evolution of the system cannot be approximated by means of the Vlasov equation.

CONCLUDING REMARKS

The stationary state for the single-waterbag distribution is shown to be a minimum-energy configuration for the one-dimensional bounded plasma with a fixed neutralizing ion background. Thus, the stationary state is not accessible for any system which is initially in a nonequilibrium state because the initial distribution has an excess of energy which cannot be accommodated by the stationary state. Numerical experiments with a one-dimensional charge-sheet model reveal the interesting property that the system does its best within the limitations of energy conservation to approach the steady state. Similar results were previously found for a one-dimensional self-gravitating system.

The minimum-energy property was extended by approximating arbitrary distribution functions by a multiple-waterbag distribution. Stationary distribution functions, which decrease monotonically in going outward from the center of the system, are found to be minimum-energy configurations and are therefore stable. The consequence of the minimum-energy property is that for arbitrary initial distributions, described by a multiple waterbag, an equilibrium state (in the Vlasov sense) is in general, inaccessible.

Langley Research Center,
National Aeronautics and Space Administration,
Langley Station, Hampton, Va., January 24, 1968,
129-02-01-01-23.

APPENDIX

MINIMUM-ENERGY PRINCIPLE FOR A SINGLE WATERBAG

In order to discuss in detail the minimum-energy property of a single-waterbag equilibrium distribution, the extremum of integrals of the form

$$W = \int_{X_1}^{X_2} g(x, V, \theta) dx \quad (A1)$$

must be considered subject to the condition that

$$N = 2A \int_{X_1}^{X_2} V dx \quad (A2)$$

is a constant. The energy density g is a known function of X , V , and θ , where $\theta = \int_{X_1}^X V(x) dx$, and X_1 and X_2 are not fixed at the outset but $V(x)$ must vanish at the end points. The positive constant A is equal to the height of the waterbag distribution function.

The purpose of this appendix is to establish the conditions that the smooth function $V(x)$, which describes the equilibrium waterbag contour, must satisfy in order that the quantity W , which is subsequently identified with the total energy of the system, shall be an extremum or, in particular, a minimum. For this purpose, the one parameter family of integrals

$$W(\epsilon) = \int_{X_1(\epsilon)}^{X_2(\epsilon)} g(x, w, \Gamma) dx \quad (A3)$$

and

$$N(\epsilon) = 2A \int_{X_1(\epsilon)}^{X_2(\epsilon)} w dx \quad (A4a)$$

are constructed, where

$$w = V(x) + \epsilon \eta(x) \quad (A4b)$$

APPENDIX

and

$$\Gamma = \theta(x) + \epsilon \zeta(x) \quad (\text{A4c})$$

The function $V(x)$ (as yet unknown) is the actual extremal curve and passes through the (as yet unknown) actual end points x_1 and x_2 ; $\eta(x)$ is an arbitrary differentiable function; ϵ is the parameter; and $\zeta(x)$ is the indefinite integral of $\eta(x)$. The trial function $w(x)$ approaches $V(x)$ as ϵ approaches zero. The intersections of a given $w(x)$ with the x -axis define the points X_1 and X_2 . As $w(x)$ approaches $V(x)$, the points X_1 and X_2 approach the actual end points x_1 and x_2 , respectively.

By the usual arguments of the calculus of variations (ref. 23), the value of $W(\epsilon)$ in equation (A3) for a given $\eta(x)$ is an extremum when ϵ is zero. In order to take the constraint equation (A4a) into proper account, the integral

$$W^*(\epsilon) = \int_{X_1(\epsilon)}^{X_2(\epsilon)} g^*(x, w, \Gamma) dx \quad (\text{A5})$$

is constructed, where $g^* = g + \lambda(2Aw)$ and λ is an as yet undetermined Lagrangian multiplier. The condition for an extremum is then

$$\left. \frac{\partial W^*(\epsilon)}{\partial \epsilon} \right|_{\epsilon=0} = 0 \quad (\text{A6})$$

With the use of equation (A5)

$$\frac{\partial W^*}{\partial \epsilon} = \frac{\partial X_2}{\partial \epsilon} g^*[X_2, w(X_2), \Gamma(X_2)] - \frac{\partial X_1}{\partial \epsilon} g^*[X_1, w(X_1), \Gamma(X_1)] + \int_{X_1}^{X_2} \left(\frac{\partial g^*}{\partial w} \frac{\partial w}{\partial \epsilon} + \frac{\partial g^*}{\partial \Gamma} \frac{\partial \Gamma}{\partial \epsilon} \right) dx \quad (\text{A7})$$

Also, $\frac{\partial w}{\partial \epsilon} = \eta$ and $\frac{\partial \Gamma}{\partial \epsilon} = \zeta$ so that by using these relations in equation (A7) and by letting $\epsilon = 0$

$$\begin{aligned} \left. \frac{\partial W^*}{\partial \epsilon} \right|_{\epsilon=0} &= \left. \frac{\partial X_2}{\partial \epsilon} \right|_{\epsilon=0} g^*[x_2, V(x_2), \theta(x_2)] - \left. \frac{\partial X_1}{\partial \epsilon} \right|_{\epsilon=0} g^*[x_1, V(x_1), \theta(x_1)] \\ &+ \int_{x_1}^{x_2} \left(\frac{\partial g^*}{\partial V} \eta + \frac{\partial g^*}{\partial \theta} \zeta \right) dx = 0 \end{aligned} \quad (\text{A8})$$

APPENDIX

The end-point conditions must be examined in detail to evaluate $\left. \frac{\partial X_2}{\partial \epsilon} \right|_{\epsilon=0}$ and $\left. \frac{\partial X_1}{\partial \epsilon} \right|_{\epsilon=0}$.

Because $w(X_1) = w(X_2) = 0$ by definition, then

$$\frac{\partial w(X_1)}{\partial \epsilon} = 0 \quad (A9)$$

for all ϵ . Thus, the use of equations (A4b) and (A4c) gives

$$\frac{\partial w(X_1)}{\partial \epsilon} = \frac{\partial w}{\partial X_1} \frac{\partial X_1}{\partial \epsilon} = V'(X_1) \frac{\partial X_1}{\partial \epsilon} + \eta(X_1) + \epsilon \eta'(X_1) = 0 \quad (A10)$$

For $\epsilon = 0$

$$V'(x_1) \left. \frac{\partial X_1}{\partial \epsilon} \right|_{\epsilon=0} + \eta(x_1) = 0$$

or

$$\left. \frac{\partial X_1}{\partial \epsilon} \right|_{\epsilon=0} = - \frac{\eta(x_1)}{V'(x_1)} \quad (A11)$$

By similar reasoning

$$\left. \frac{\partial X_2}{\partial \epsilon} \right|_{\epsilon=0} = - \frac{\eta(x_2)}{V'(x_2)} \quad (A12)$$

Substitution of equations (A11) and (A12) into equation (A8) and use of integration by parts in the first integral of equation (A8) gives

$$\begin{aligned} & - \frac{g^*[x_2, V(x_2), \theta(x_2)]}{V'(x_2)} \eta(x_2) + \frac{g^*[x_1, V(x_1), \theta(x_1)]}{V'(x_1)} \eta(x_1) + \zeta \left. \frac{\partial g^*}{\partial V} \right|_{x_1}^{x_2} \\ & + \int_{x_1}^{x_2} \left[\frac{\partial g^*}{\partial \theta} - \frac{d}{dx} \left(\frac{\partial g^*}{\partial V} \right) \right] \zeta dx = 0 \end{aligned} \quad (A13)$$

Equation (A13) must hold for a rather wide class of functions $\eta(x)$ and $\zeta(x)$. In particular, equation (A13) must hold for those functions $\zeta(x)$ which are nonzero but are

APPENDIX

compatible with $\zeta(x_1) = \zeta(x_2) = \eta(x_1) = \eta(x_2) = 0$. For such a case

$$\frac{\partial g^*}{\partial \theta} - \frac{d}{dx} \left(\frac{\partial g^*}{\partial V} \right) = 0 \quad (A14)$$

Again, η can be nonzero at one end point but zero at the other end point when ζ vanishes at both end points, and so forth. By this method

$$\frac{g^*[x_2, V(x_2), \theta(x_2)]}{V'(x_2)} = 0 \quad (A15)$$

$$\frac{g^*[x_1, V(x_1), \theta(x_1)]}{V'(x_1)} = 0 \quad (A16)$$

$$\left. \frac{\partial g^*}{\partial V} \right|_{x=x_1} = 0 \quad (A17)$$

and

$$\left. \frac{\partial g^*}{\partial V} \right|_{x=x_2} = 0 \quad (A18)$$

Equations (A14) to (A18) and the original constraint equation (A2) with x_1 and x_2 replacing X_1 and X_2 , respectively, are the equations used to determine $V(x)$, x_1 , x_2 , and λ .

The function $g(x, V, \theta)$ for specializing to the case of the single waterbag is now introduced. The total energy per unit length of the waterbag $g(x, V, \theta)$ is given by

$$\int \frac{1}{2} m v^2 f \, dv + \frac{\epsilon_f E^2}{2} = \int_{-V(x)}^{V(x)} A \left(\frac{1}{2} m v^2 \right) dv + \frac{\epsilon_f}{2} E^2$$

where

$$\begin{aligned} E &= \frac{e}{\epsilon_f} \int_{x_1}^x \left\{ n_0 \left[H(x + x_1) - H(x - x_1) \right] - 2AV(x) \right\} dx \\ &= \frac{en_0}{\epsilon_f} \left\{ x \left[H(x + x_1) - H(x - x_1) \right] + x_1 \left[H(x + x_1) - H(x - x_1) \right] \right\} - \frac{2e}{\epsilon_f} A \theta \end{aligned} \quad (A19)$$

APPENDIX

Then

$$g^*(x, V, \theta) = g + 2A\lambda V = \frac{Am}{3} V^3 + \frac{\epsilon_f}{2} \left(\frac{en_0}{\epsilon_f} \left\{ x \left[H(x + x_1) - H(x - x_1) \right] + x_1 \left[H(x + x_1) - H(x - x_1) \right] \right\} - \frac{2e}{\epsilon_f} A\theta \right)^2 + 2A\lambda V \quad (A20)$$

Use of equation (A20) in equations (A17) and (A18) gives

$$\lambda = 0 \quad (A21)$$

where $V(x_1) = V(x_2) = 0$. For finite $V'(x_1)$ and $V'(x_2)$, equations (A15) and (A16) require that

$$g^*[x_1, V(x_1), \theta(x_1)] = g^*[x_2, V(x_2), \theta(x_2)] = 0 \quad (A22)$$

Use of equations (A20), (A21), and (A2) shows that the relations in equation (A22) are identically satisfied. Equation (A14) now reduces to

$$\frac{\partial g}{\partial \theta} - \frac{d}{dx} \left(\frac{\partial g}{\partial V} \right) = 0 \quad (A23)$$

The use of equations (A19) and (A20) in equation (A23) gives the differential equation

$$V \frac{dV}{dx} + \frac{eE}{m} = 0 \quad (A24)$$

which must be satisfied by $V(x)$. Equation (A24) and the constraint equation

$$N = 2A\theta(x_2) \quad (A25)$$

are sufficient to determine x_1 , x_2 , and $V(x)$ where $V(x_1) = V(x_2) = 0$.

By noting that $\theta \rightarrow \theta$ and $V = \frac{d\theta}{dx} \rightarrow \theta'$ transform equation (A14) into the customary Euler-Lagrange equation, the Legendre test (ref. 22) may now be applied to the second variation of the integral W^* . The Legendre test states that in order for the

APPENDIX

solution $V(x)$ of equation (A24) to be such that the integral W^* is maximized, the quantity

$$\frac{\partial^2 g^*}{\partial V^2} = 2AmV$$

must be negative definite over the interval from x_1 to x_2 . This quantity is seen to be positive definite over the interval so that the extremum represented by $V(x)$ cannot be a maximum, but must be either a minimum or a simple inflection. Other evidence presented herein indicates that the extremum is a minimum.

REFERENCES

1. Buneman, O.: Dissipation of Currents in Ionized Media. *Phys. Rev., Second ser.*, vol. 115, no. 3, Aug. 1, 1959, pp. 503-517.
2. Buneman, O.: Maintenance of Equilibrium by Instabilities. *J. Nucl. Energy: Pt. C*, vol. 2, Jan. 1961, pp. 119-134.
3. Dunn, D. A.; and Ho, I. T.: Computer Experiments on Ion-Beam Neutralization With Initially Cold Electrons. Rep. No. 0309-1 (Contract AF33(616)-7944), Stanford Electron. Lab., Stanford Univ., Apr. 1963.
4. Birdsall, Charles K.; and Bridges, William B.: Space-Charge Instabilities in Electron Diodes and Plasma Converters. *J. Appl. Phys.*, vol. 32, no. 12, Dec. 1961, pp. 2611-2618.
5. Bridges, William B.; and Birdsall, Charles K.: Space-Charge Instabilities in Electron Diodes. II. *J. Appl. Phys.*, vol. 34, no. 10, Oct. 1963, pp. 2946-2955.
6. Smith, Craig; and Dawson, John: Some Computer Experiments With a One-Dimensional Plasma Model. MATT-151 (Contract No. AT(30-1)-1238), Plasma Phys. Lab., Princeton Univ., Jan. 1963.
7. Burger, P.; Dunn, D. A.; and Halsted, A. S.: Computer Experiments on the Randomization of Electrons in a Collisionless Plasma. *Phys. Fluids*, vol. 8, no. 12, Dec. 1965, pp. 2263-2272.
8. Derfler, Heinrich: Nonexistence of Quiescent Plasma States in Ion Propulsion. *Phys. Fluids*, vol. 7, no. 10, Oct. 1964, pp. 1625-1637.
9. Hasegawa, Akira; and Birdsall, Charles K.: Sheet-Current Plasma Model for Ion-Cyclotron Waves. *Phys. Fluids*, vol. 7, no. 10, Oct. 1964, pp. 1590-1600.
10. Burger, Peter: Theory of Large-Amplitude Oscillations in the One-Dimensional Low-Pressure Cesium Thermionic Converter. *J. Appl. Phys.*, vol. 36, no. 6, June 1965, pp. 1938-1943.
11. Burger, Peter: The Opposite-Stream Plasma Diode. Rep. No. 0254-1 (NASA Grant NsG 299-63), Stanford Electron. Lab., Stanford Univ., Apr. 1964.
12. Auer, P. L.; Hurwitz, H., Jr.; and Kilb, R. W.: Low Mach Number Magnetic Compression Waves in a Collision-Free Plasma. *Phys. Fluids*, vol. 4, no. 9, Sept. 1961, pp. 1105-1121.
13. Auer, P. L.; Hurwitz, H., Jr.; and Kilb, R. W.: Large-Amplitude Magnetic Compression of a Collision-Free Plasma. II. Development of a Thermalized Plasma. *Phys. Fluids*, vol. 5, no. 3, Mar. 1962, pp. 298-316.

14. Rossow, Vernon J.: Magnetic Compression of Collision-Free Plasmas With Charge Separation. *Phys. Fluids*, vol. 8, no. 2, Feb. 1965, pp. 358-366.
15. Dawson, John: One-Dimensional Plasma Model. *Phys. Fluids*, vol. 5, no. 4, Apr. 1962, pp. 445-459.
16. Dawson, John M.: Thermal Relaxation in a One-Species, One-Dimensional Plasma. *Phys. Fluids*, vol. 7, no. 3, Mar. 1964, pp. 419-425.
17. Eldridge, O. C.; and Feix, M.: Numerical Experiments With a Plasma Model. *Phys. Fluids*, vol. 6, no. 3, Mar. 1963, pp. 398-406.
18. Eldridge, O. C.; and Feix, M.: One-Dimensional Plasma Model at Thermodynamic Equilibrium. *Phys. Fluids*, vol. 5, no. 9, Sept. 1962, pp. 1076-1080.
19. Eldridge, O.; and Feix, M.: Fokker-Planck Coefficients for a One-Dimensional Plasma. *Phys. Fluids*, vol. 5, no. 10, Oct. 1962, pp. 1307-1308.
20. DePackh, D. C.: The Water-Bag Model of a Sheet Electron Beam. *J. Electron. Contr.*, First ser., vol. XIII, no. 5, Nov. 1962, pp. 417-424.
21. Hohl, Frank; and Feix, Marc R.: Numerical Experiments With a One-Dimensional Model for a Self-Gravitating Star System. *Astrophys. J.*, vol. 147, no. 3, Mar. 1967, pp. 1164-1180.
22. Courant, R.; and Hilbert, D.: *Methods of Mathematical Physics. Vol. I.* Interscience Publ., Inc. (New York), 1953.
23. Forsyth, A. R.: *Calculus of Variations.* Cambridge Univ. Press, 1927, pp. 1-48.

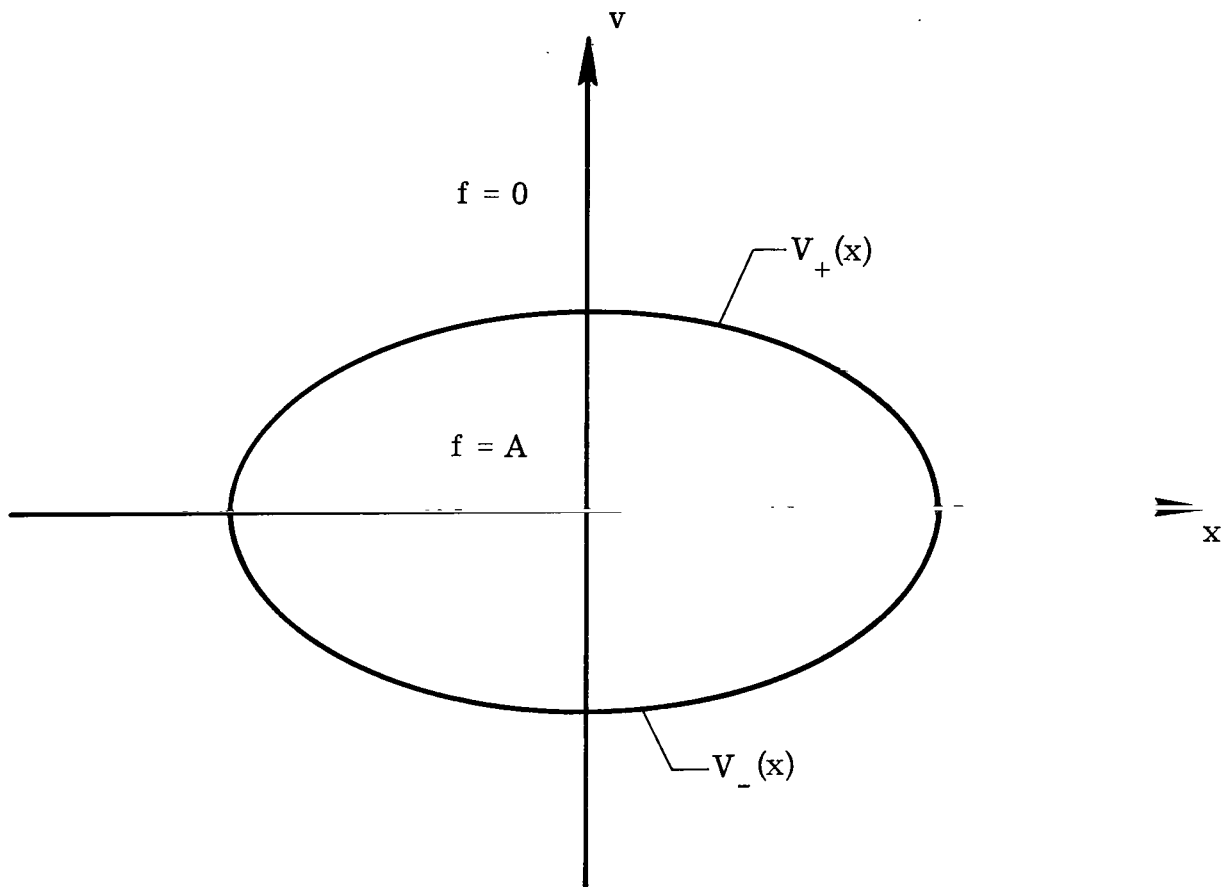


Figure 1.- Waterbag distribution.

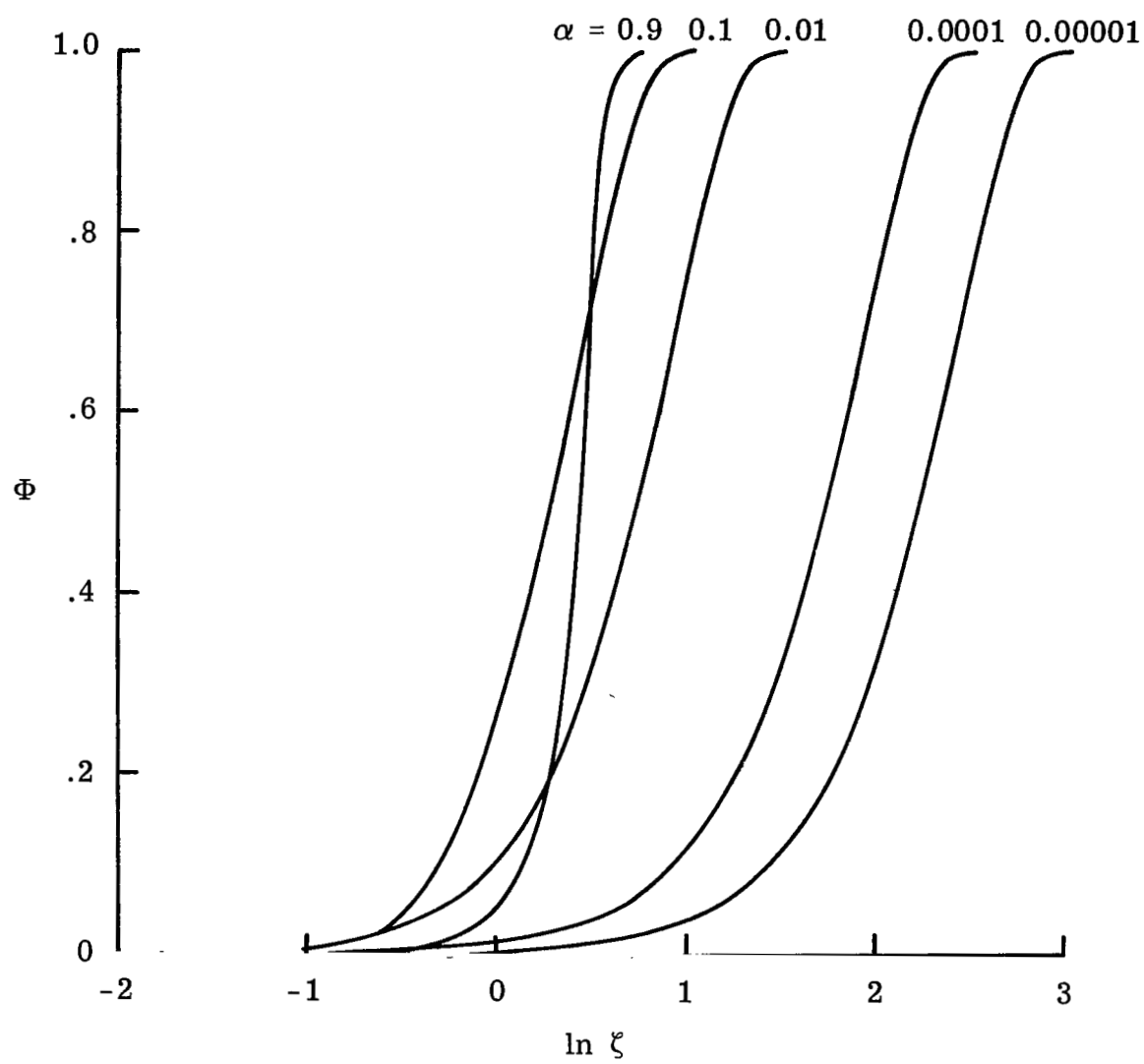


Figure 2.- Variation of the dimensionless potential as a function of $\ln \zeta$ for several values of α .

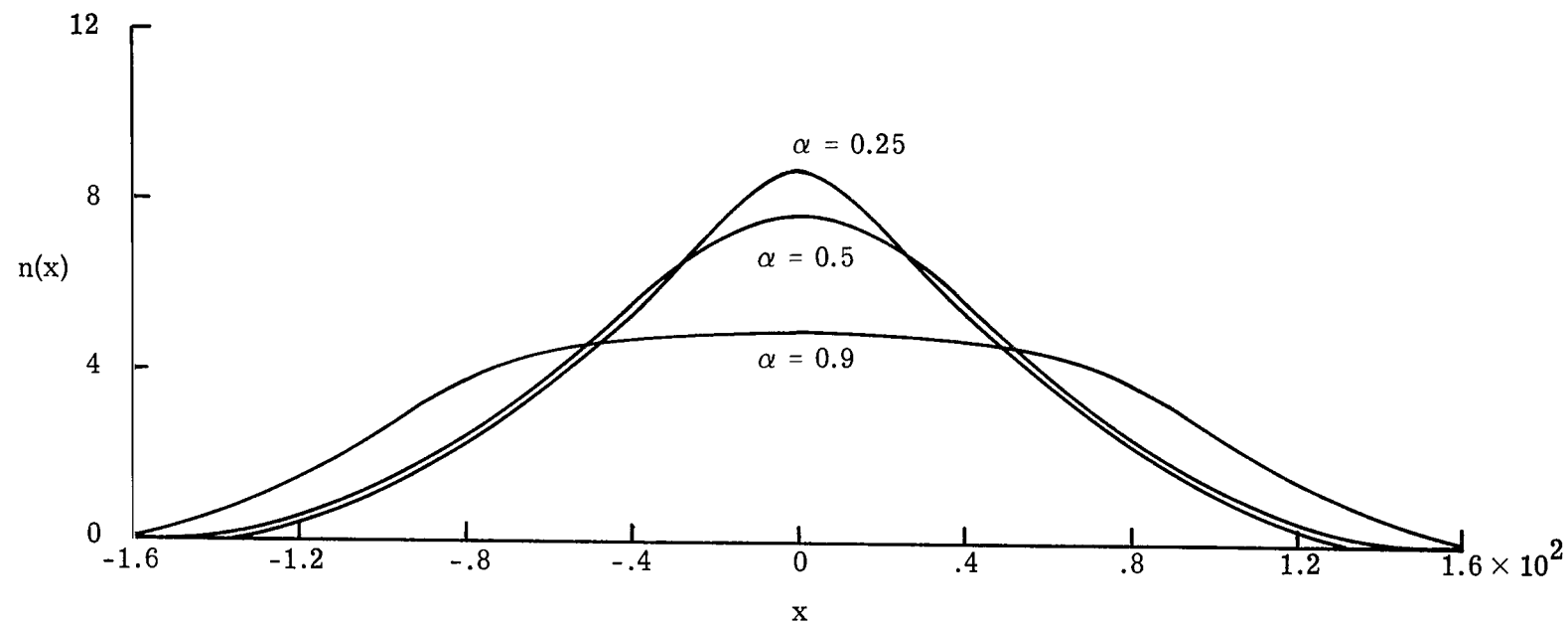


Figure 3.- Variation of electron density for several values of α .

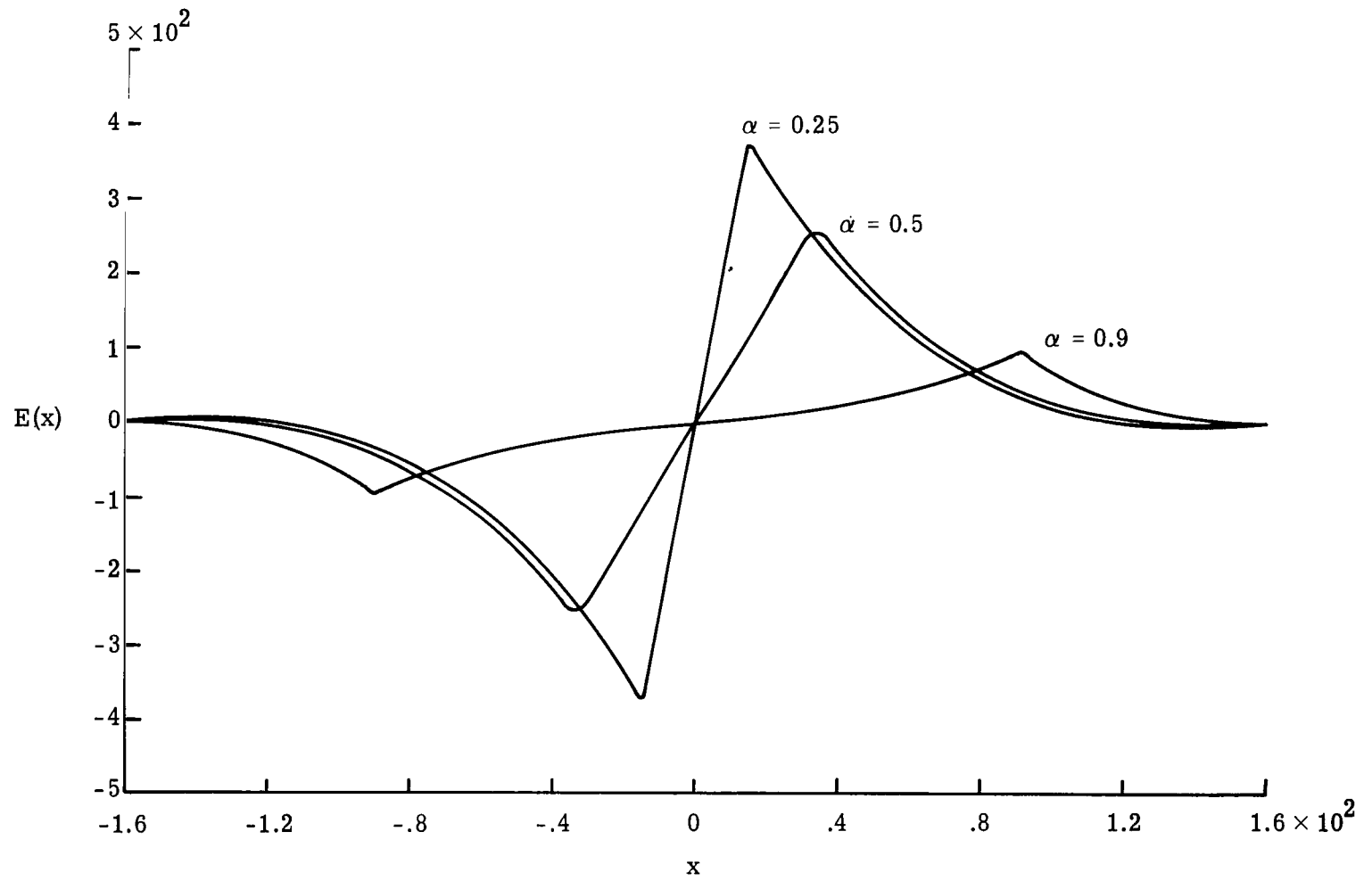


Figure 4.- Variation of the electric field for several values of α .

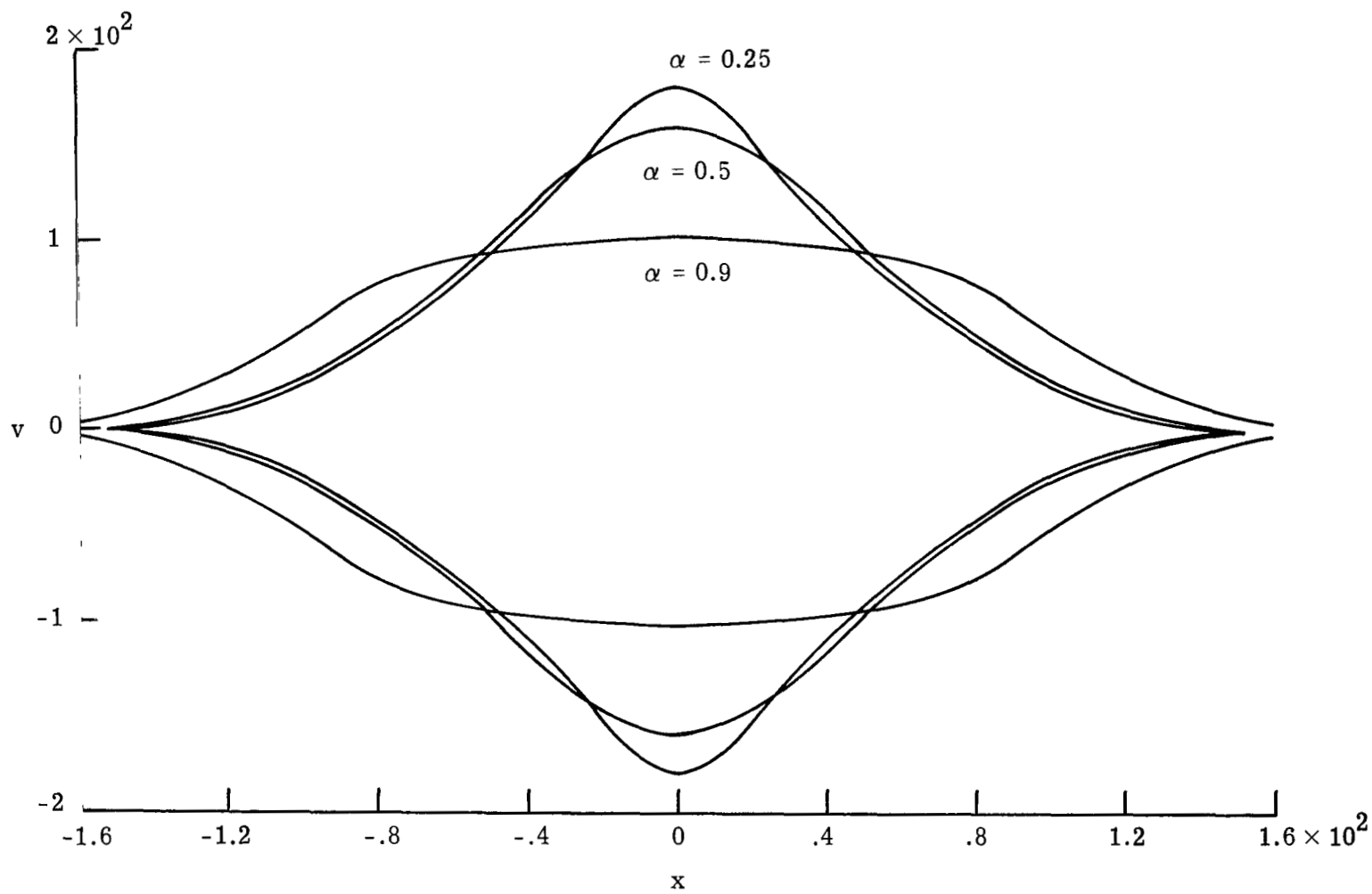


Figure 5.- Equilibrium waterbag contours for several values of α .

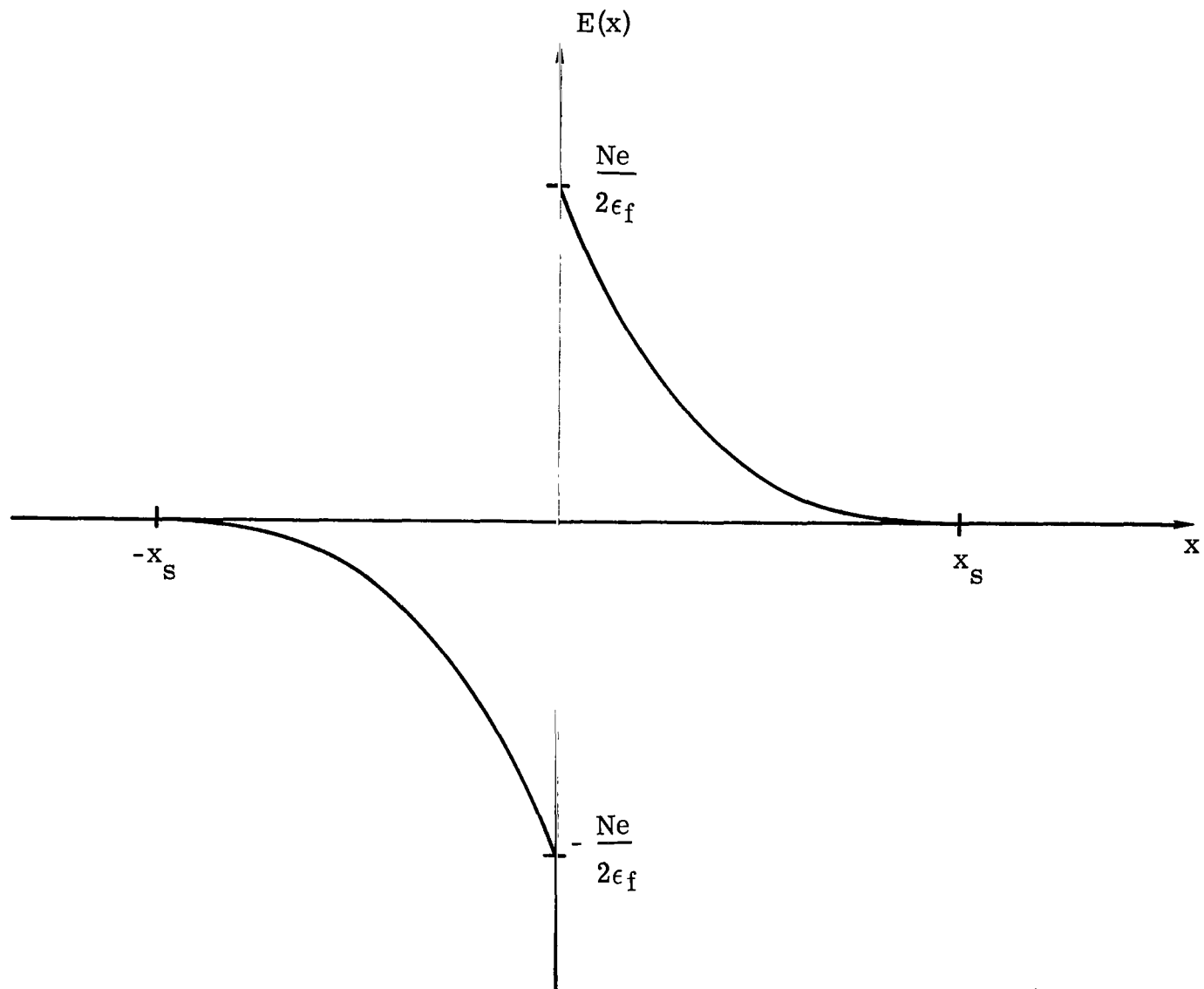


Figure 6.- Variation of the electric field for a positively charged grid.

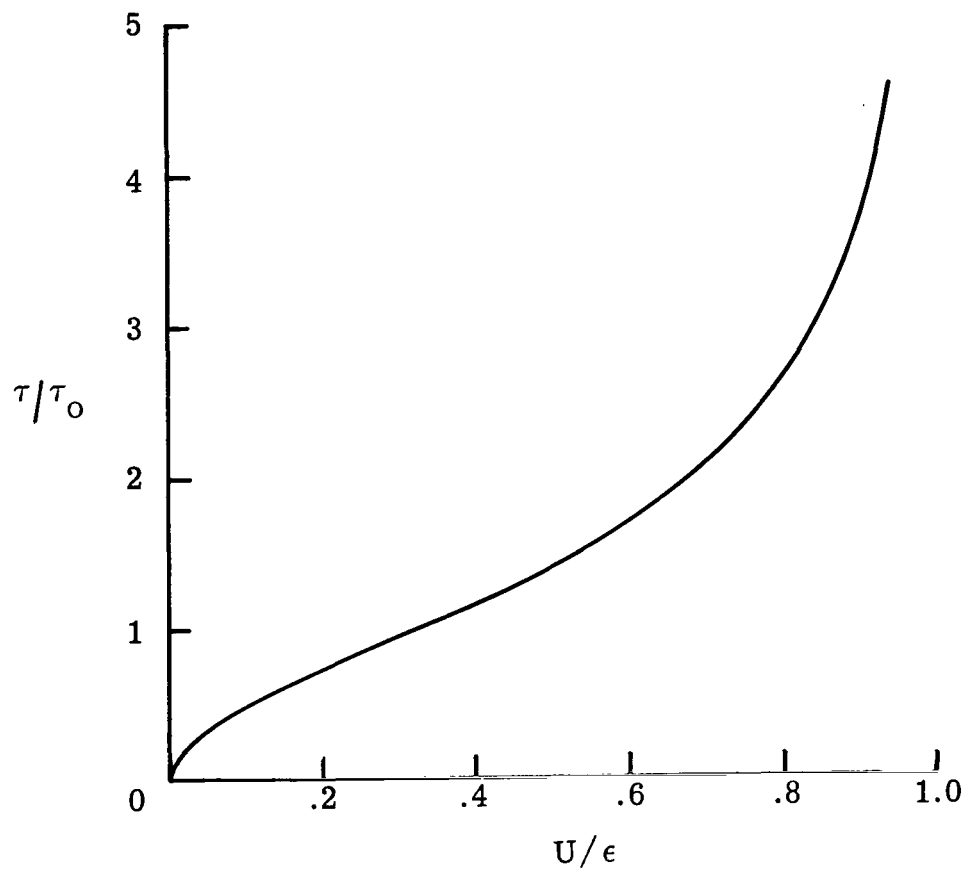


Figure 7.- Variation of electron period with energy.

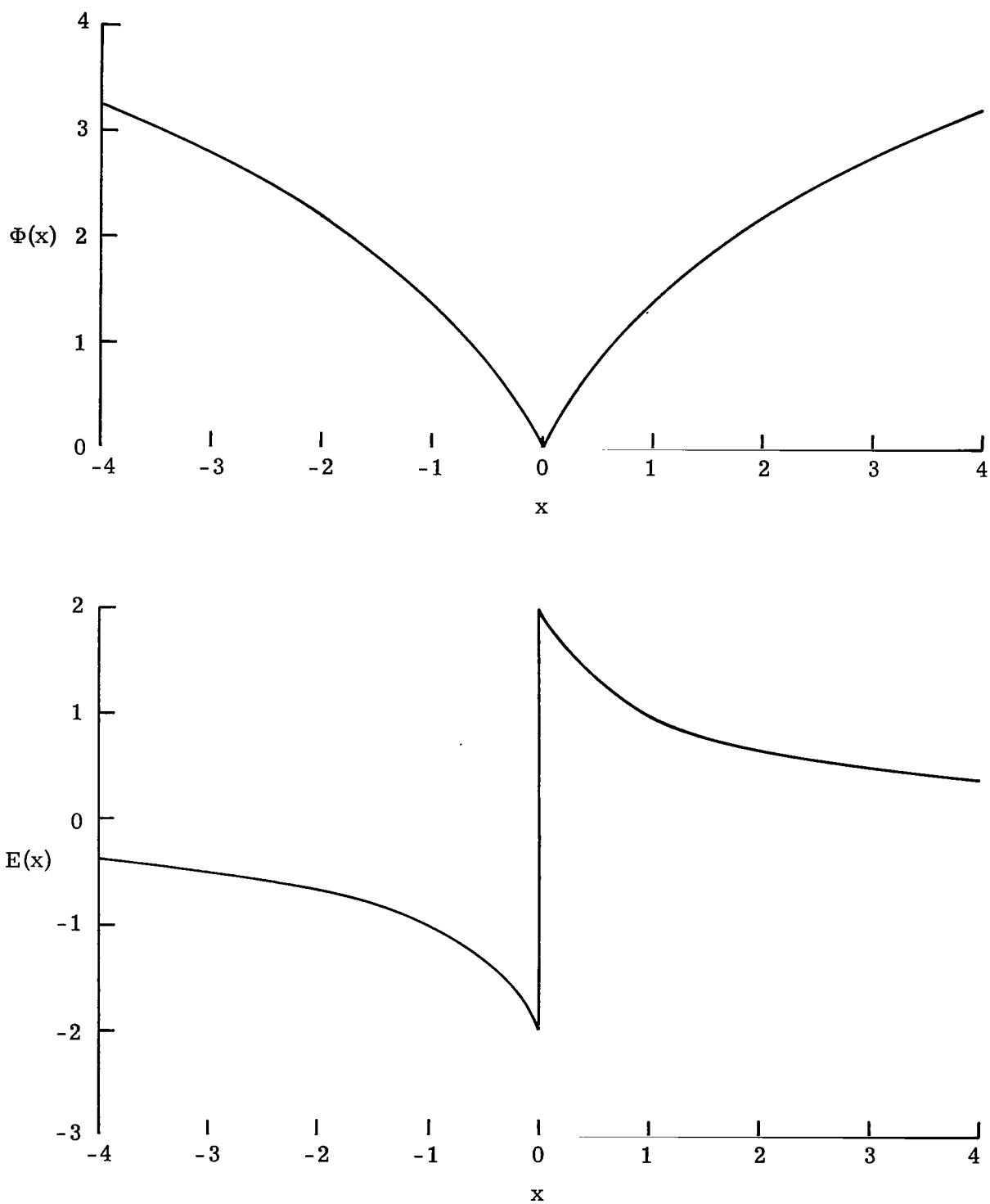


Figure 8.- Variation of the potential and electric field near a positively charged grid for a Maxwellian velocity distribution.

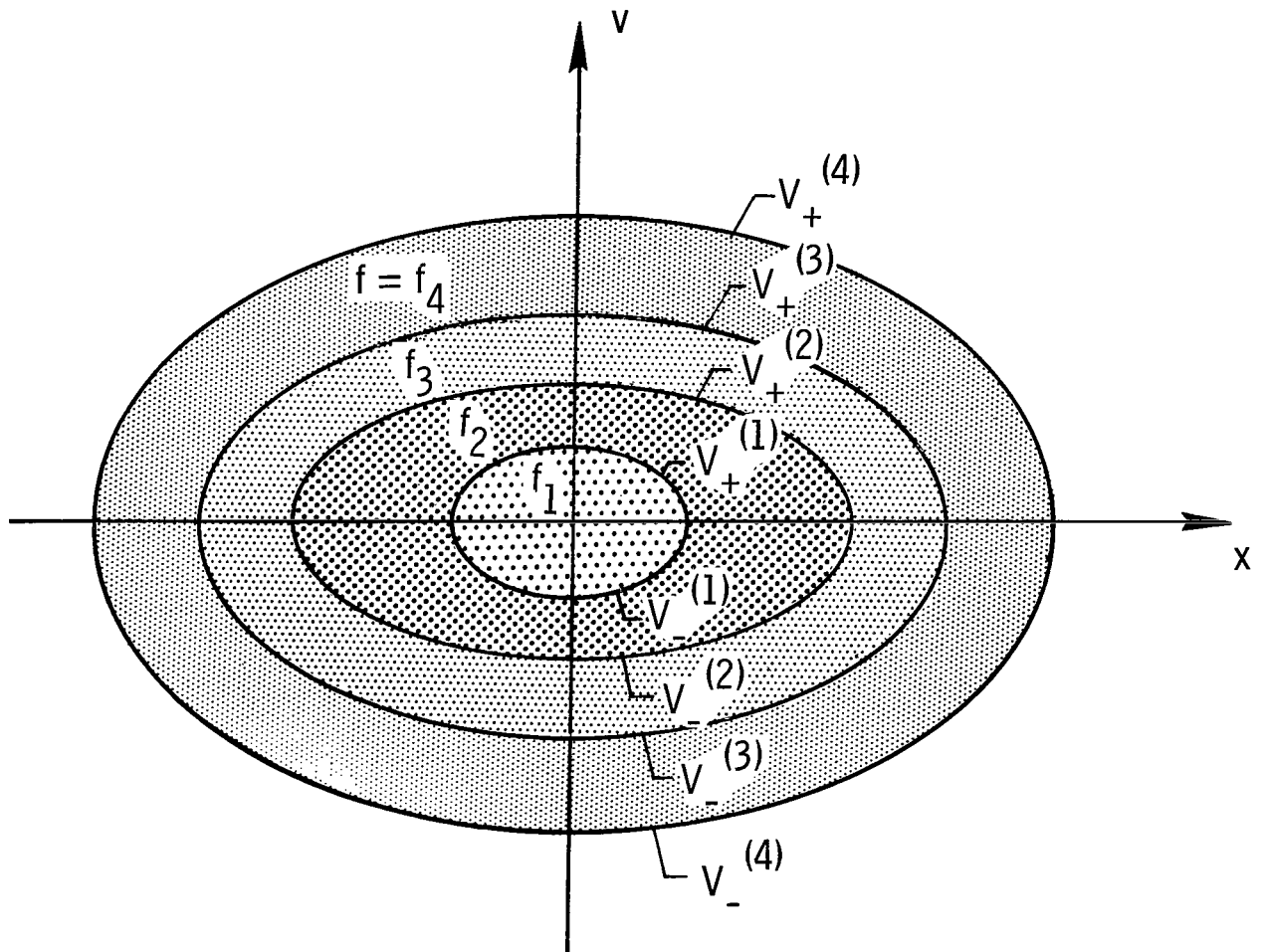


Figure 9.- Illustration of a multiple-contour-waterbag distribution.

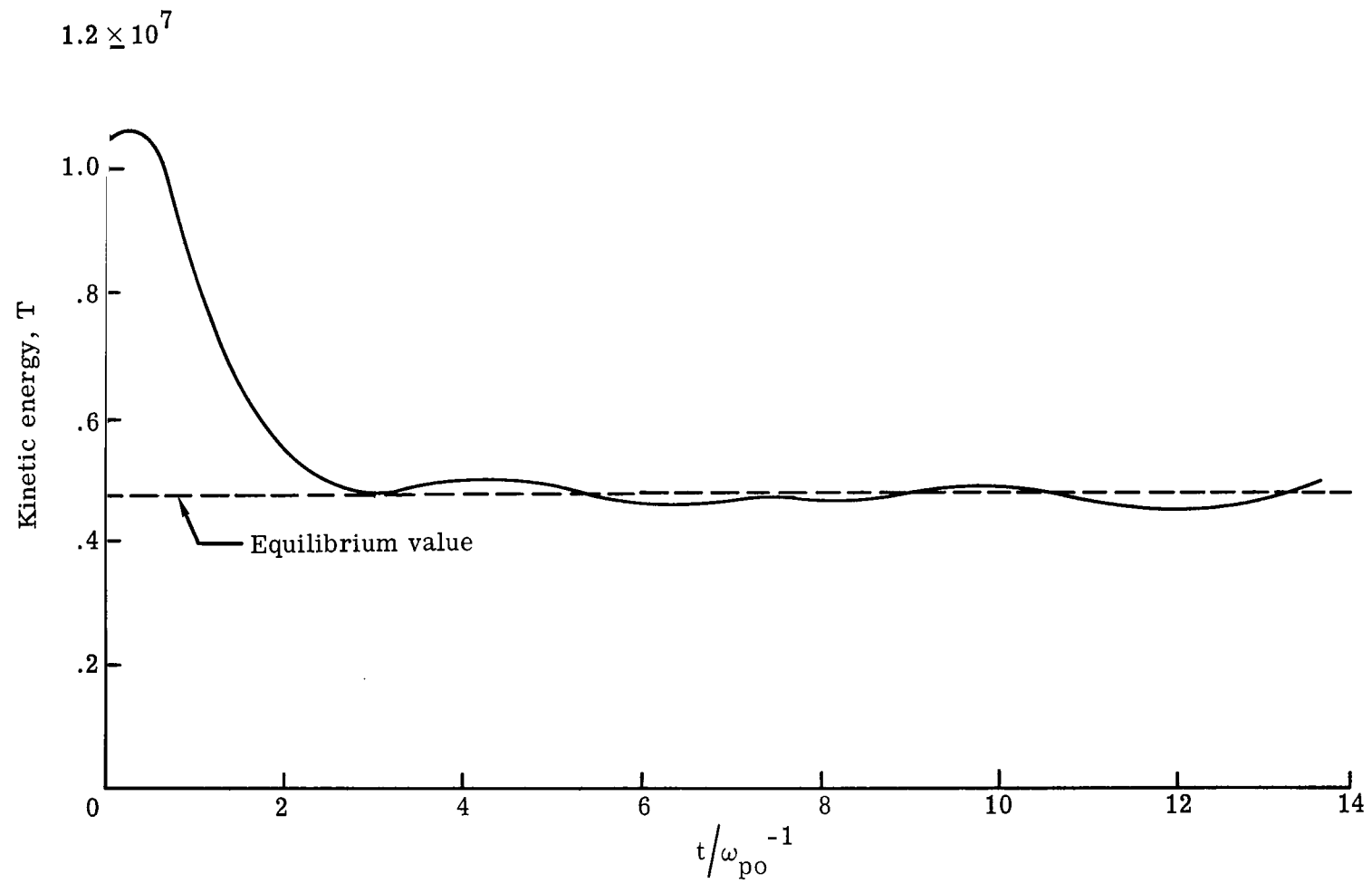


Figure 10.- Variation of kinetic energy for a 1000-electron system near equilibrium.

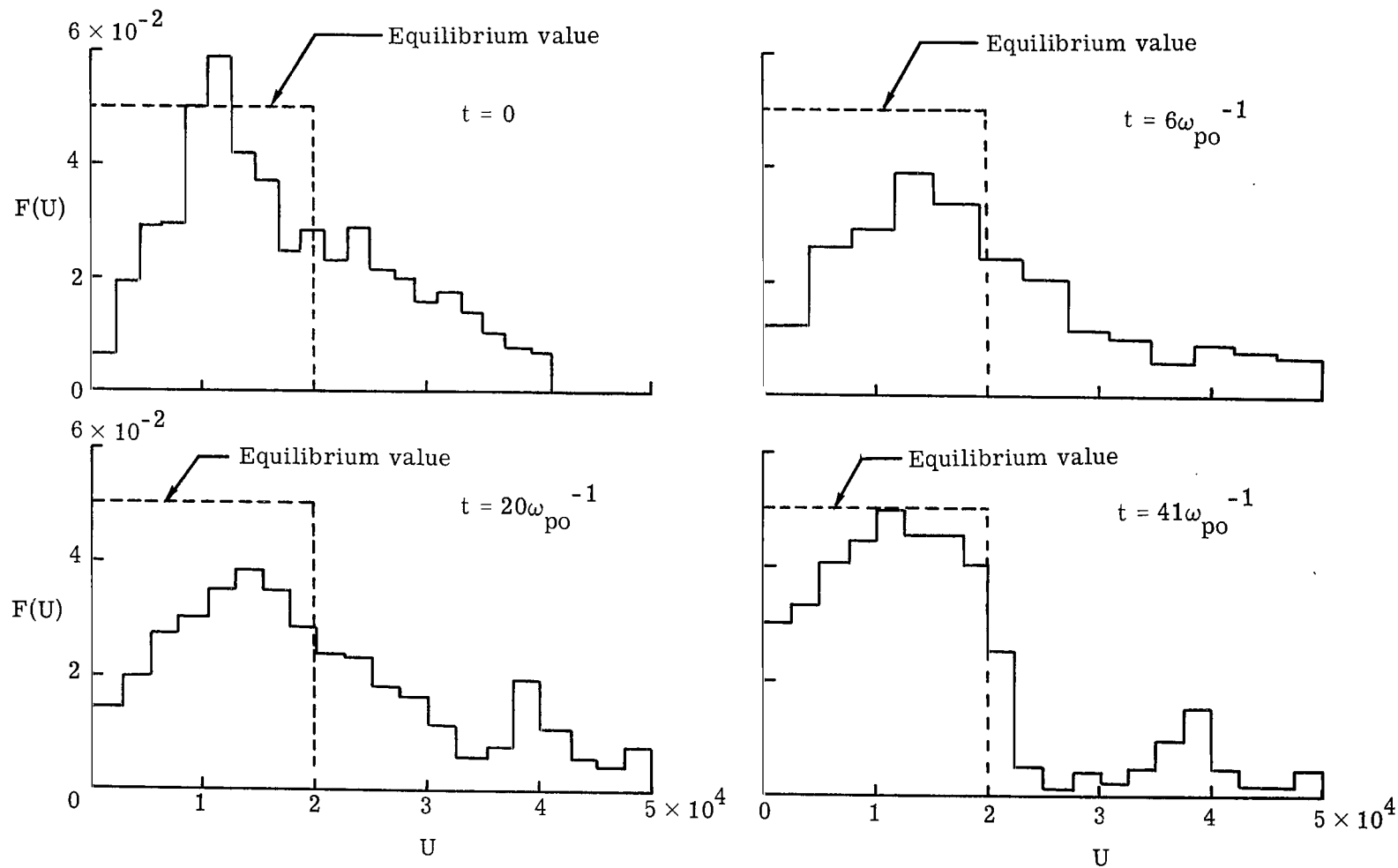


Figure 11.- Time development of the energy distribution function for a 1000-electron system near equilibrium.

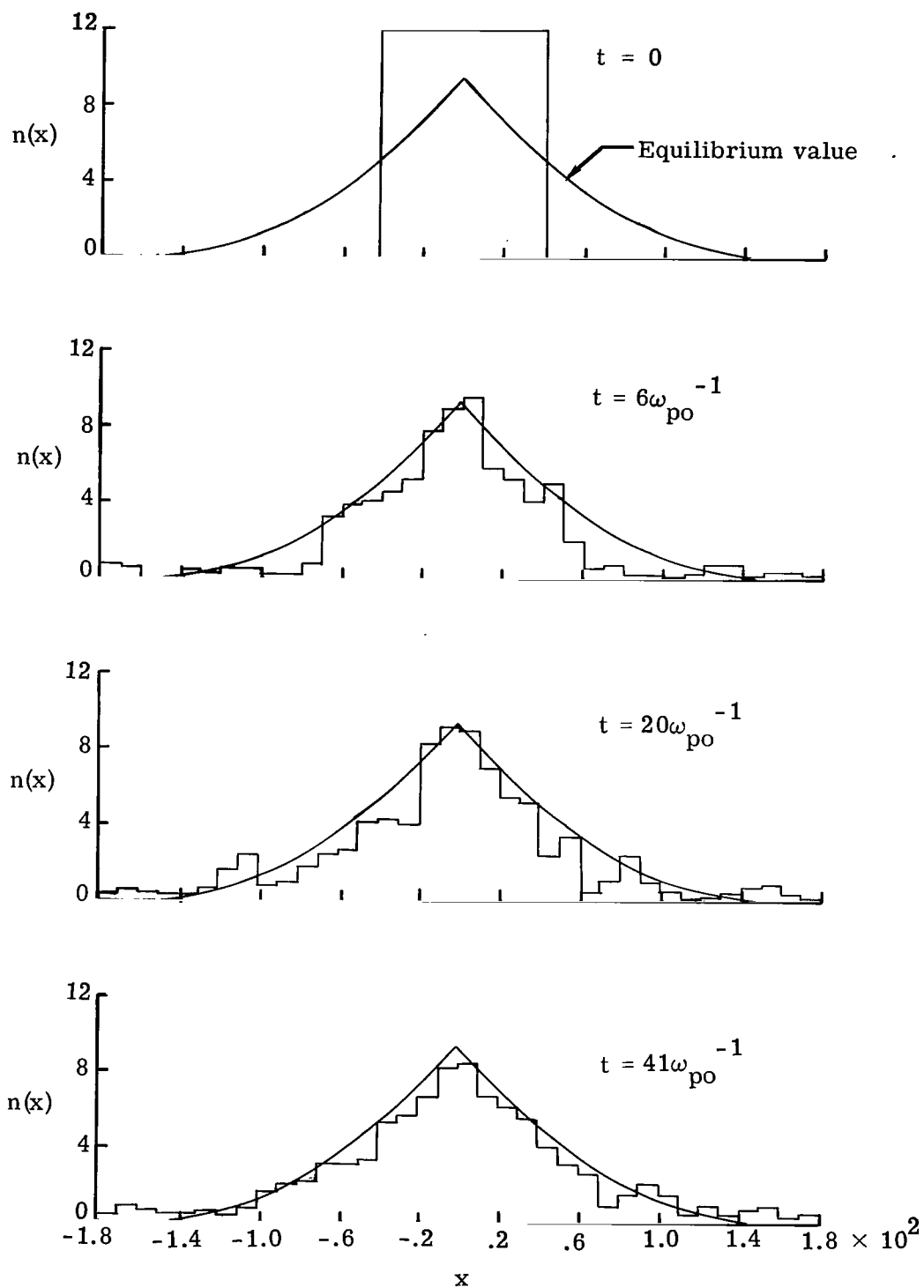


Figure 12.- Time development of the density for a 1000-electron system near equilibrium.

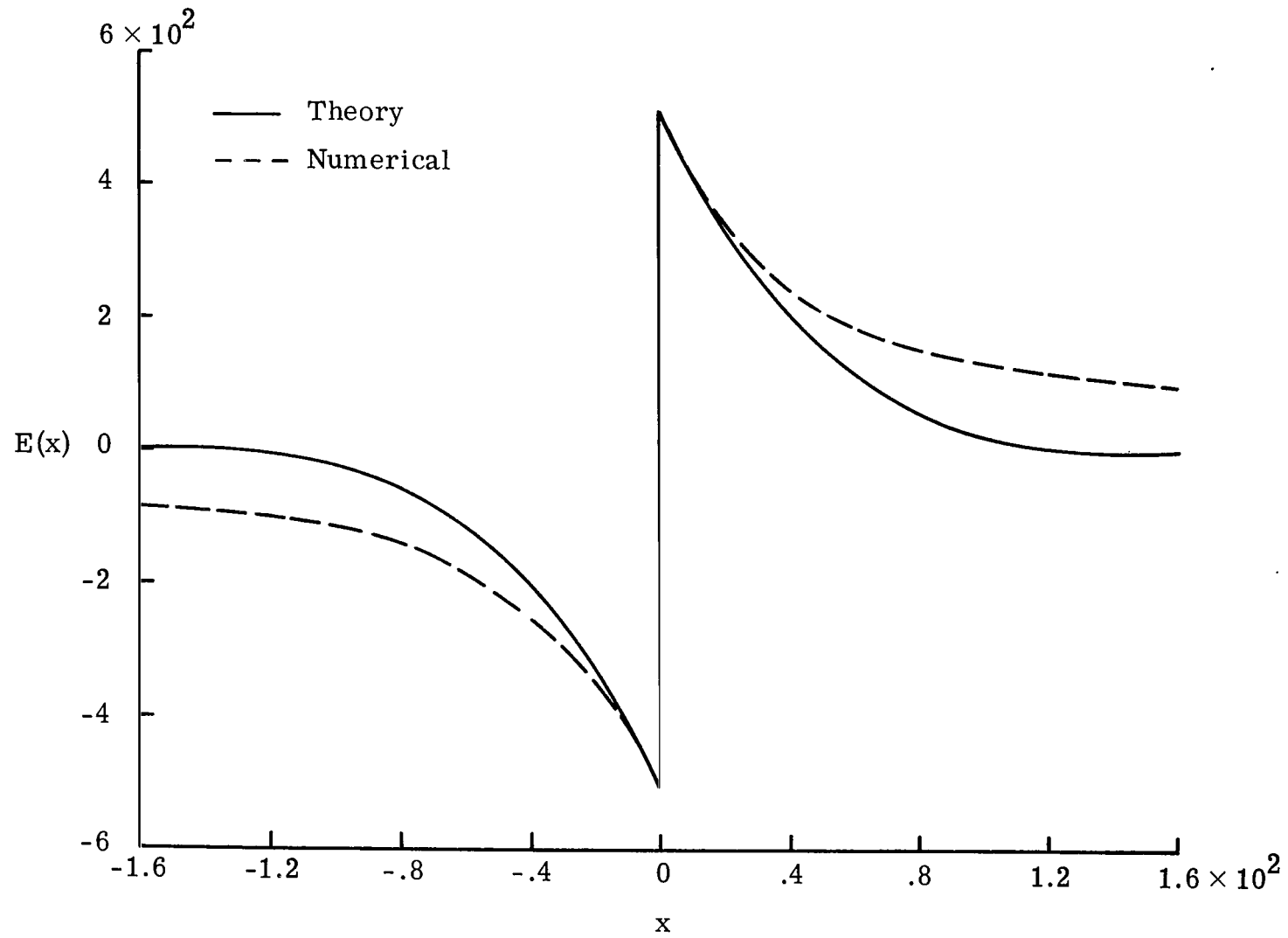
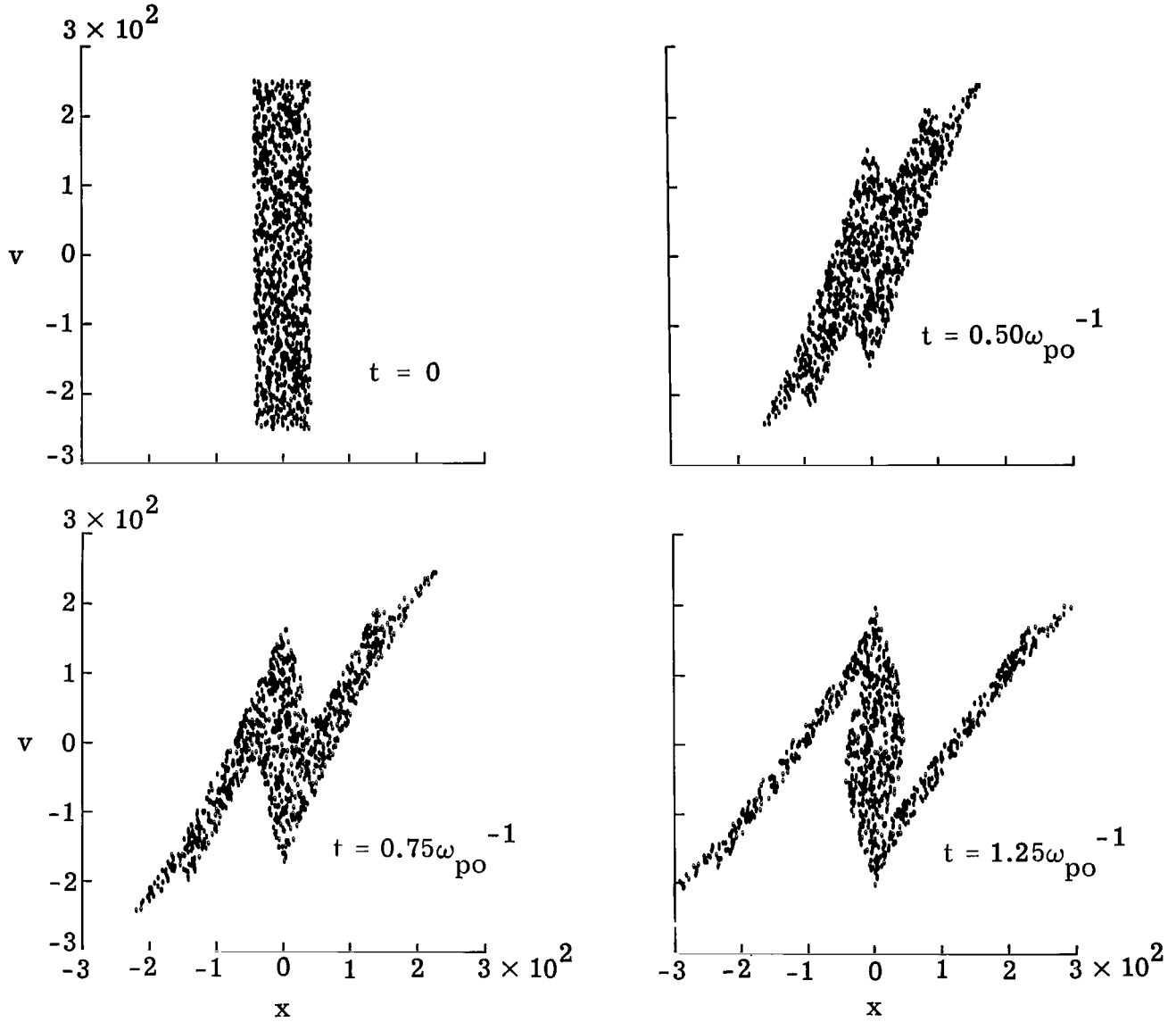
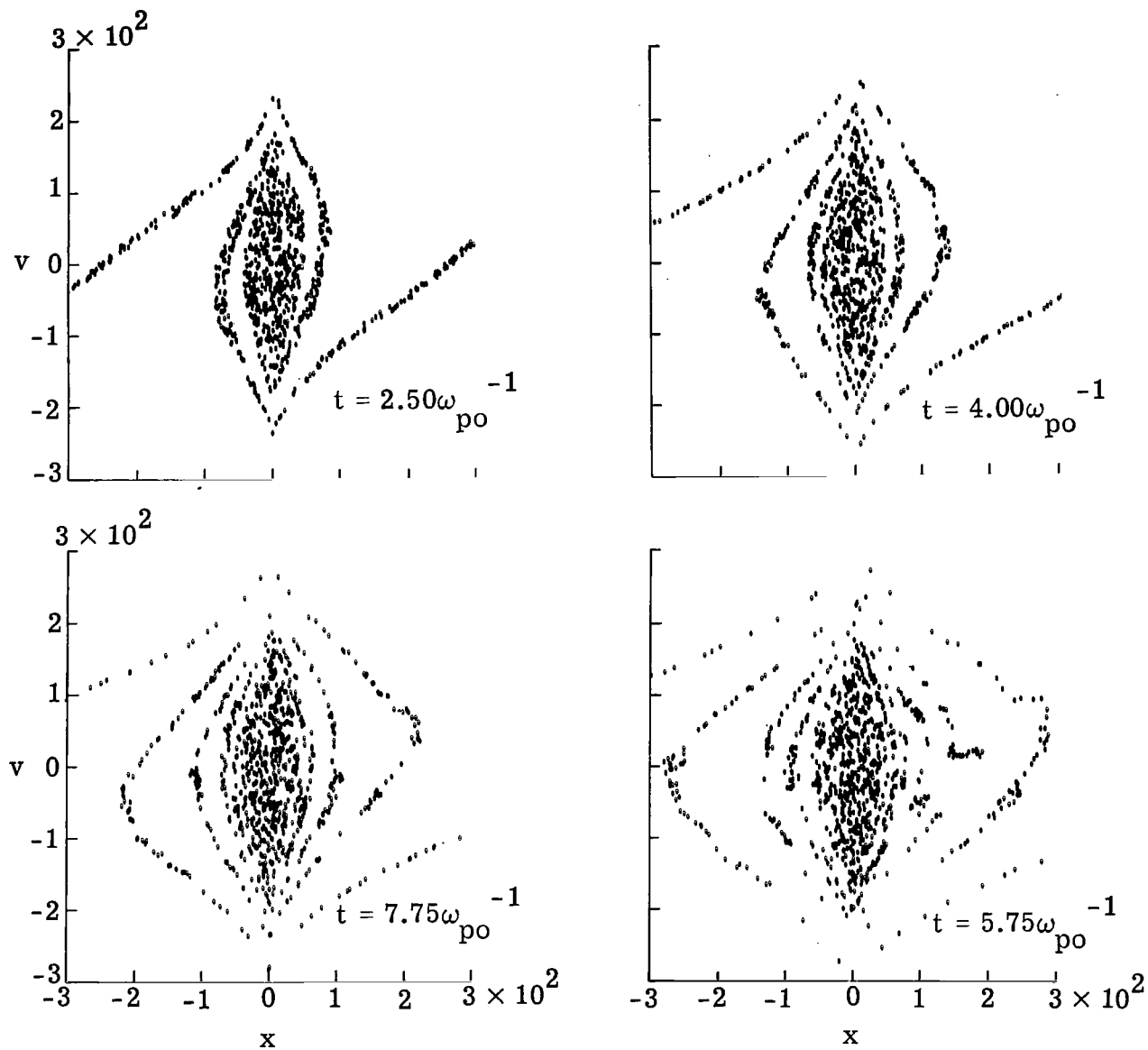


Figure 13.- Comparison of the experimental electric field with the theoretical or equilibrium value.



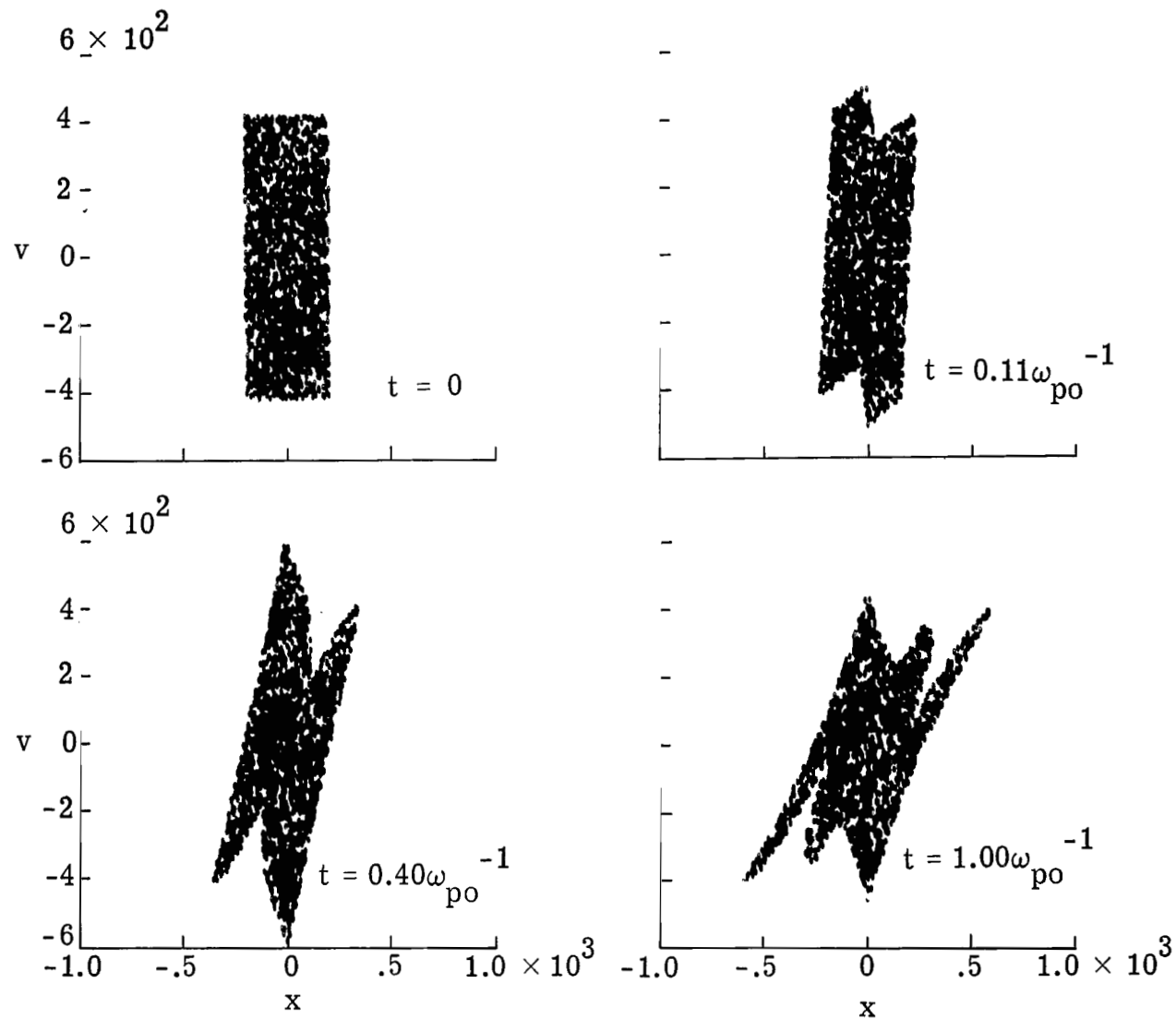
(a) Time development from $t = 0$ to $t = 1.25\omega_{po}^{-1}$.

Figure 14.- Time development in phase space for a 1000-electron system near equilibrium.



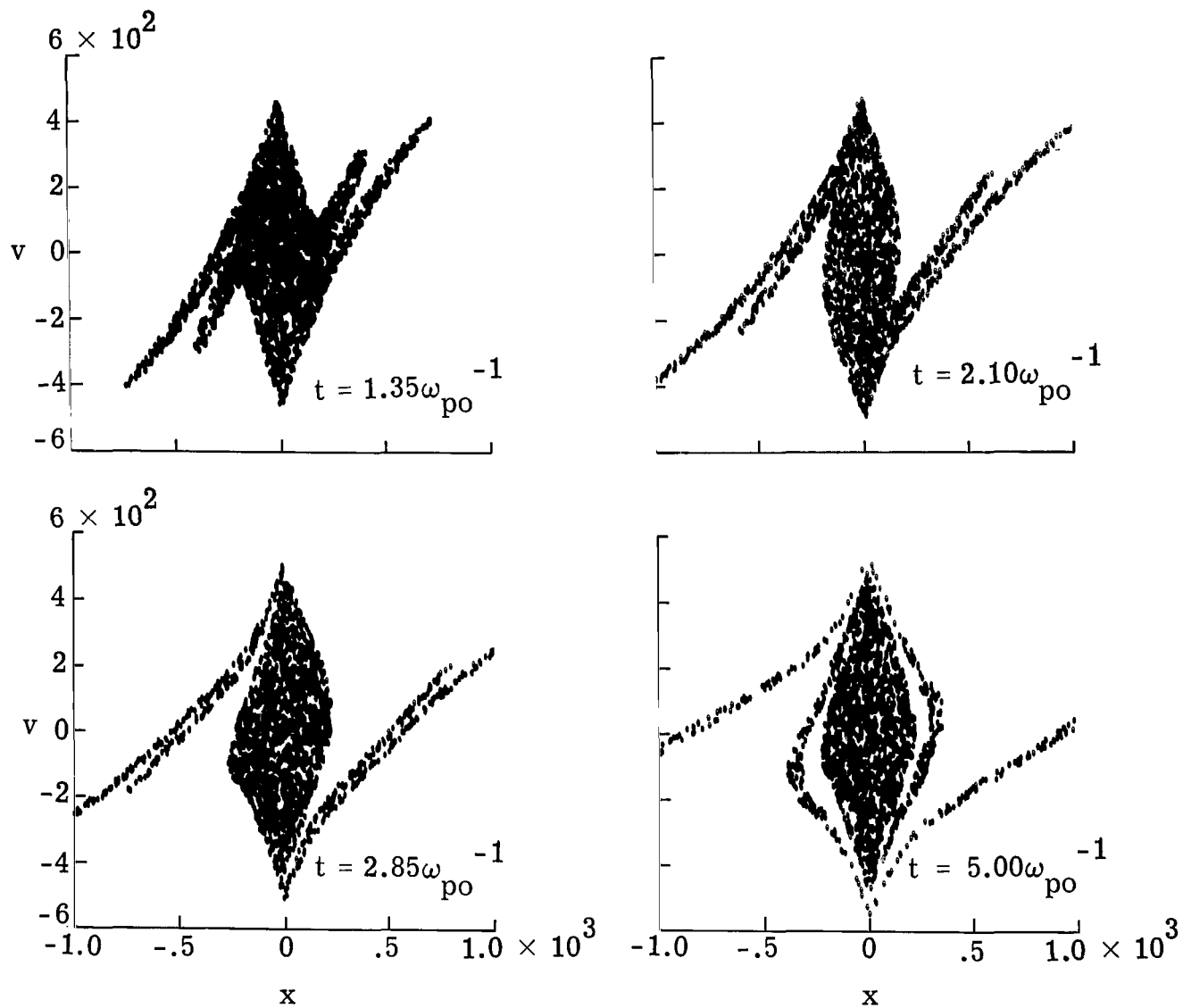
(b) Time development from $t = 2.50\omega_{po}^{-1}$ to $t = 5.75\omega_{po}^{-1}$.

Figure 14.- Concluded.



(a) Time development from $t = 0$ to $t = 1.00\omega_{po}^{-1}$.

Figure 15.- Time development in phase space of a 2000-electron system near equilibrium.



(b) Time development from $t = 1.35\omega_{po}^{-1}$ to $t = 5.00\omega_{po}^{-1}$.

Figure 15.- Concluded.

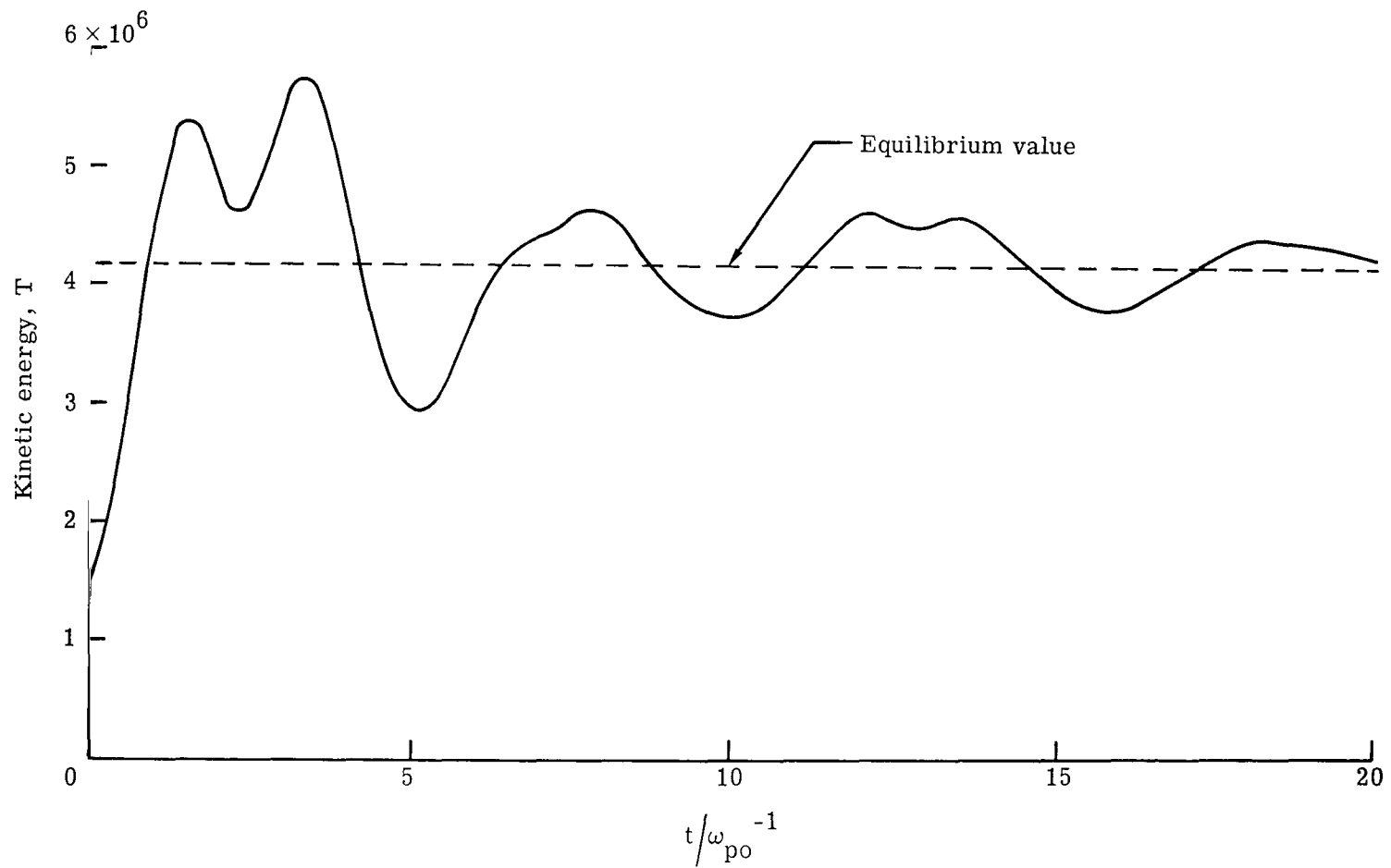


Figure 16.- Variation of kinetic energy for a collision-dominated system with $x_i = 477$.

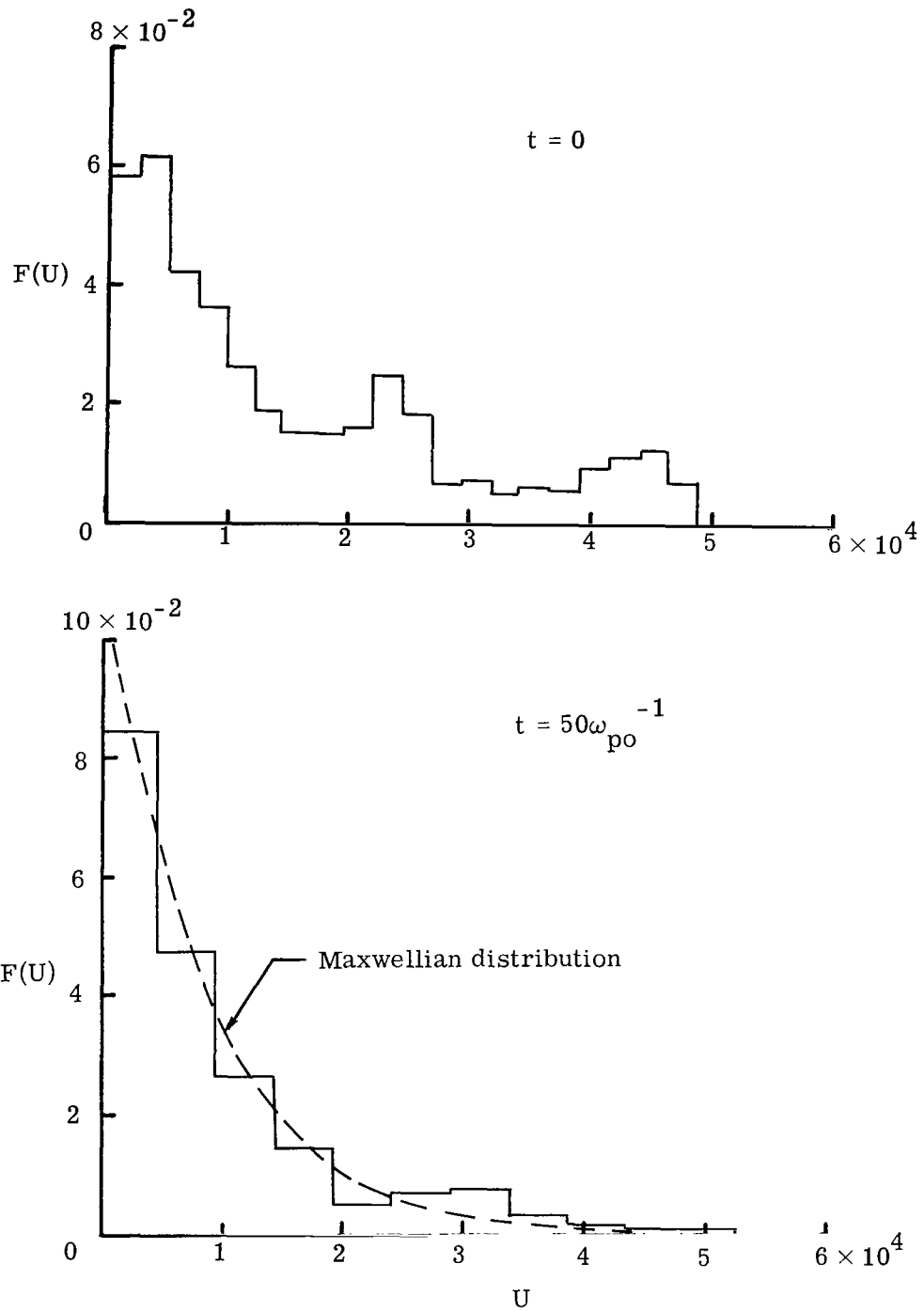
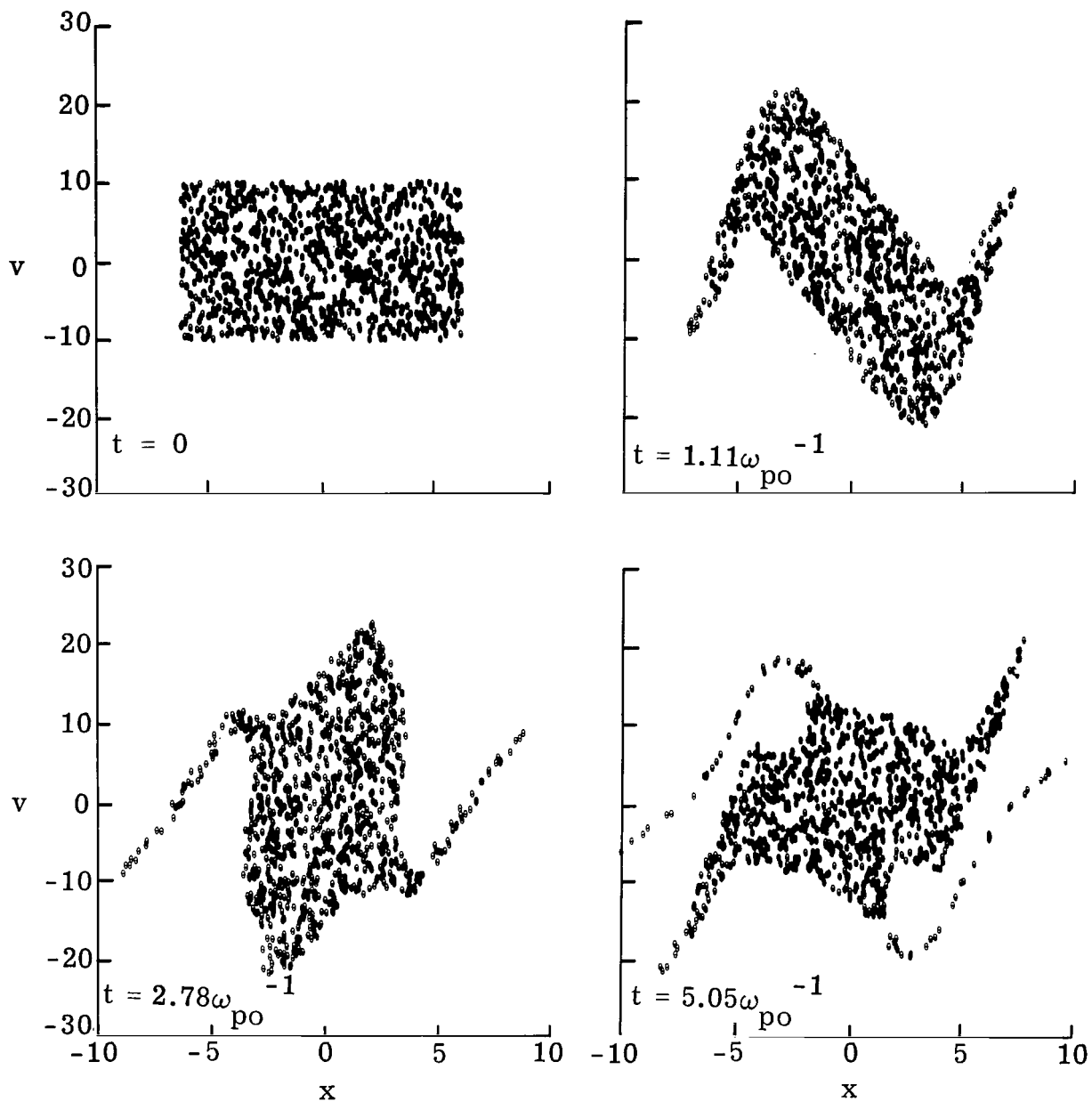
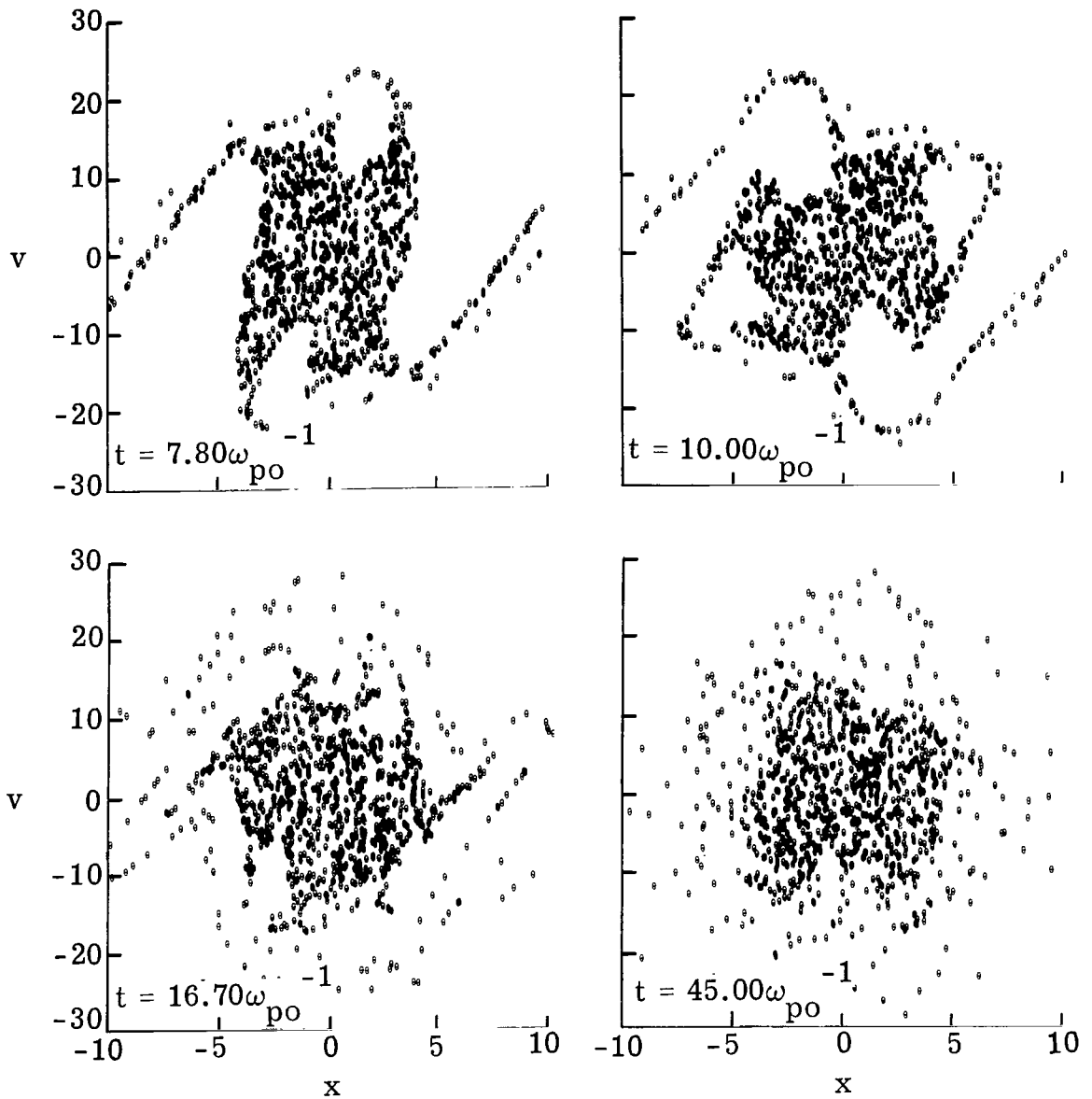


Figure 17.- Time development of the energy distribution function for a collision-dominated system with $x_1 = 477$.



(a) Time development from $t = 0$ to $t = 5.05\omega_{po}^{-1}$.

Figure 18.- Time development in phase space for a 1000-electron collision-dominated system.



(b) Time development from $t = 7.80 \omega_{po}^{-1}$ to $t = 45.00 \omega_{po}^{-1}$.

Figure 18.- Concluded.

POSTMASTER: If Undeliverable (Section 15
Postal Manual) Do Not Return

"The aeronautical and space activities of the United States shall be conducted so as to contribute . . . to the expansion of human knowledge of phenomena in the atmosphere and space. The Administration shall provide for the widest practicable and appropriate dissemination of information concerning its activities and the results thereof."

— NATIONAL AERONAUTICS AND SPACE ACT OF 1958

NASA SCIENTIFIC AND TECHNICAL PUBLICATIONS

TECHNICAL REPORTS: Scientific and technical information considered important, complete, and a lasting contribution to existing knowledge.

TECHNICAL NOTES: Information less broad in scope but nevertheless of importance as a contribution to existing knowledge.

TECHNICAL MEMORANDUMS: Information receiving limited distribution because of preliminary data, security classification, or other reasons.

CONTRACTOR REPORTS: Scientific and technical information generated under a NASA contract or grant and considered an important contribution to existing knowledge.

TECHNICAL TRANSLATIONS: Information published in a foreign language considered to merit NASA distribution in English.

SPECIAL PUBLICATIONS: Information derived from or of value to NASA activities. Publications include conference proceedings, monographs, data compilations, handbooks, sourcebooks, and special bibliographies.

TECHNOLOGY UTILIZATION PUBLICATIONS: Information on technology used by NASA that may be of particular interest in commercial and other non-aerospace applications. Publications include Tech Briefs, Technology Utilization Reports and Notes, and Technology Surveys.

Details on the availability of these publications may be obtained from:

SCIENTIFIC AND TECHNICAL INFORMATION DIVISION
NATIONAL AERONAUTICS AND SPACE ADMINISTRATION
Washington, D.C. 20546